

Research Paper

VeloceGenomics: An Accelerated *in Vivo* Drug Discovery Approach to Rapidly Predict the Biologic, Drug-Like Activity of Compounds, Proteins, or Genes

Ruben Papoian,¹ Andreas Scherer,¹ Muriel Saulnier,¹ Frank Staedtler,¹ André Cordier,¹ Francois Legay,¹ Gerard Maurer,¹ Joerg Staeheli,¹ Jacky Vonderscher,¹ and Salah-Dine Chibout^{1,2}

Received April 18, 2005; accepted June 22, 2005

Purpose. The aim of this study is to test the predictive power of *in vivo* multiorgan RNA expression profiling in identifying the biologic activity of molecules.

Methods. Animals were treated with compound A or B. At the end of the treatment period, *in vivo* multiorgan microarray-based gene expression data were collected. Investigators masked to the identity of the compounds analyzed the transcriptome signatures to define the molecular pathways affected by treatment and to hypothesize the biologic activity and potential therapeutic indications of the blinded compounds.

Results. For compound A, G-protein-coupled receptors and factors associated with cell growth were affected—growth hormone/insulin-like growth factor-1, glucagon/insulin axes, and general somatostatin-like activity. Deblinding showed the compound to be a somatostatin analog, SOM230, confirming the accuracy of the predicted biologic activity. For compound B, components of the inflammatory cascade potentially mediated by lipopolysaccharide, tumor necrosis factor, or proinflammatory cytokines were affected. The gene expression signatures were most consistent with an interleukin-6 family activity. Deblinding revealed that compound B was leukemia inhibitory factor.

Conclusions. VeloceGenomics is a strategy of coupling *in vivo* compound testing with genomic technologies. The process enables prediction of the mechanism of action and, coupled with other relevant data, prediction of the suitability of compounds for advancement in the drug development process.

KEY WORDS: *in vivo* compound profiling; *in vivo* RNA expression profiling; mechanism of action; microarray; pharmacogenomics.

INTRODUCTION

Because of the analytic power of gene expression studies, microarray technology has become an integral part of the drug discovery and drug development processes (1). This has been possible to a great extent because microarray experiments can measure simultaneously the expression of thousands of genes. Gene expression profiling in the phar-

maceutical industry is applied in studies of toxicology, target identification, and validation and has become an integral component of drug discovery and the preclinical phase of drug development (2–4).

The traditional drug discovery process is based on screening chemicals or biologic products, in an *in vitro*, high-throughput mode, against a battery of defined, preselected drug targets (e.g., enzymatic reactions, ligand–receptor interactions) (5). The use of *in vitro* models for screening compound activity has proven to be successful because the complexity of the biologic response is reduced and focused onto specific cell types and molecular targets. However, the weakness of this approach is the “artificially disconnected” use of *in vitro* target models that do not reflect the tightly interconnected and interdependent relationships of the different targets that exist in a whole organism (5–7). Another drawback is that the biologic activity against all nonselected targets is missed. Therefore, the full biologic consequences—beneficial or detrimental—are not fully revealed. Drug discovery research strategies that introduce *in vivo* studies early in the process and truly validate the full pharmacologic activity of potentially interesting compounds can circumvent many of the pitfalls of early-stage research (4,8–11). An investigative approach that integrates molecular information

¹Department of Exploratory Development, Biomarker Development, Novartis Pharma A.G., Postfach, 4002, Basel, Switzerland.

²To whom correspondence should be addressed. (e-mail: salahdine.chibout@novartis.com)

ABBREVIATIONS: AMPA, α -amino-3-hydroxy-5-methyl-4-isoxazolepropionic acid; ERK, extracellular signal-related kinase; GH, growth hormone; GPCR, G-protein-coupled receptor; IGF, insulin-like growth factor; IL, interleukin; JAK, Janus kinase; LIF, leukemia inhibitory factor; LPS, lipopolysaccharide; LRR, leucine-rich repeats; MAPK, mitogen-activated protein kinase; NF- κ B, nuclear factor kappa beta; OSM, oncostatin M; PI3K, phosphatidylinositol 3 kinase; SOCS, suppressor of cytokine signaling; SSTR, somatostatin receptors; STAT, signal transducer and activator of transcription; TIMP, tissue inhibitor of metalloproteinase; TLR, Toll-like receptor; TRAF, tumor necrosis factor receptor-associated factor.

(e.g., gene expression profiling) on the actions of a compound throughout an organism may provide a more efficient and effective solution to the challenges of pharmacologic efficacy and safety evaluation in complex biologic systems.

We describe an approach to the drug discovery process that we have termed *VeloceGenomics*, an accelerated drug discovery strategy for predicting the biologic, drug-like function of a molecule using *in vivo* multiorgan whole transcriptome analyses (organism-wide gene expression profiling). This strategy may be used irrespective of the molecular target or the therapeutic indication. *In vivo* testing is the only accepted approach that can bring understanding of the full pharmacologic, toxicologic, and therapeutic potential of a compound under evaluation (10,11).

We tested the capability of this strategy to produce a compound-specific, multiorgan molecular signature through a series of blinded evaluations of two well-characterized proteins. The results demonstrated that through careful analysis of the gene expression profile, data miners working on the coded samples were able to predict the pharmacologic activities, most of the potential therapeutic indications, potential adverse effects, and protein family of the blinded compounds. This comprehensive approach, used early in the drug discovery process, should allow more accurate risk assessment of a compound's potential for drug development success.

MATERIALS AND METHODS

Outline of the VeloceGenomics Process

The VeloceGenomics process is outlined in Fig. 1. A gene (cDNA), protein, small molecule, or other type of compound is selected for analysis. The animals may be otherwise healthy, naive animals, or they may be specifically bred or engineered as disease models. Appropriate route of administration, dose, treatment schedule, and treatment duration are established. At the end of treatment, RNA is extracted from multiple organs, glands, and tissues. The primary data captured after treatment are the multiorgan RNA expression profiles. However, this information can be supplemented with a vast array of additional assays during and at the end of treatment (e.g., hematology or clinical biochemistry). Data mining and analysis are performed to enable prediction of the most plausible mode(s) of action, therapeutic indications, safety concerns, and issues that would affect the decision to promote a compound for further testing or commercial development.

Origin of Tissue, Treatments, and Tissue Processing

In this study, purpose-bred male and female cynomolgus monkeys (*Macaca fascicularis*), each approximately 24 months of age and weighing approximately 3 kg, were used. The monkeys were bred at the Centre de Recherches Primatologiques, Port Louis, Mauritius. At the breeder's facilities, the monkeys were treated against parasitic arthropods and helminths and subjected to a program of tuberculin testing.

The *in vivo* phase of this study was conducted at CIT (Evreux, France). On arrival at CIT, each animal was given a complete clinical examination under the supervision of a

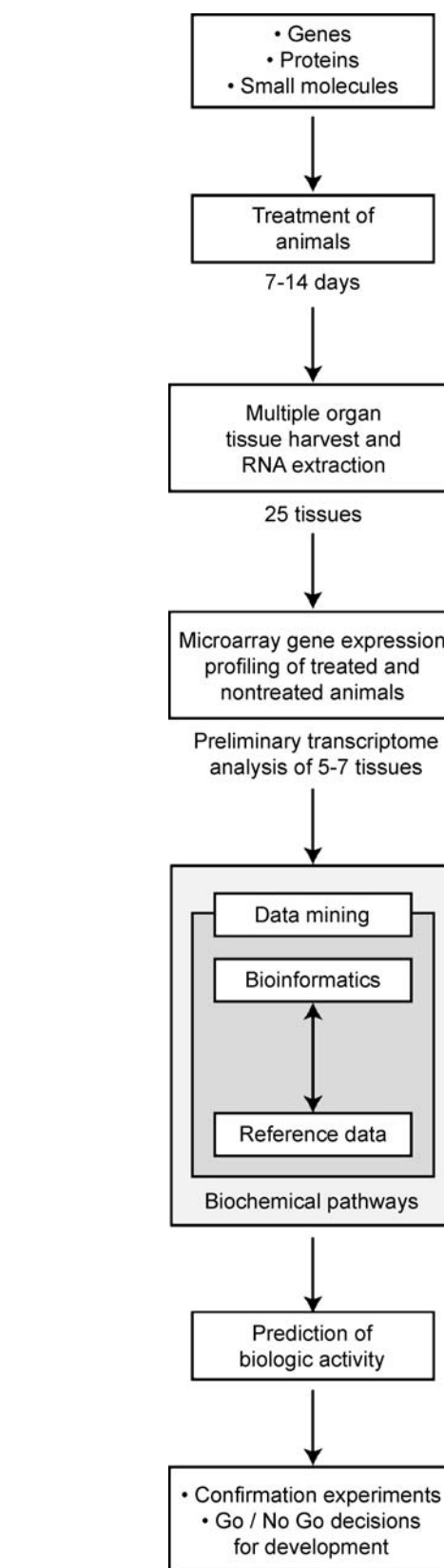


Fig. 1. Outline of the VeloceGenomics process.

veterinarian. Anthelmintic treatment was administered. Coprologic examination and tuberculin testing were performed. The animals were held in quarantine for at least 3 weeks.

After quarantine, they were acclimated to the study conditions for at least 5 days before treatment began. The animals were individually identified by chest or thigh tattoo from the breeder's facility and by a unique CIT identity number given at the beginning of the study.

From their arrival at CIT, the animals were housed in a dedicated primate unit. The animal room conditions were set as follows: temperature, $24 \pm 3^\circ\text{C}$; relative humidity, $50 \pm 20\%$; light/dark cycle, 12 h each (0700–1900 h); ventilation, approximately 12 cycles/h of filtered, nonrecycled air. The corresponding instrumentation and equipment were checked and calibrated at regular intervals. Temperature and relative humidity were recorded continuously, and records were checked daily and filed.

All animals had free access to tap water (filtered with a 0.22- μm filter). Approximately 200 g of UAR 107 C pelleted diet (UAR; Villemoisson, Epinay-sur-Orge, France) was distributed daily to each animal. The food was given at least 1 h after dosing on the days of treatment. In addition, two fruits or vegetables were given daily to each animal.

The study was conducted in compliance with the following French Animal Health regulation: Council Directive No. 86/609/EEC of 24th November 1986 on the harmonization of laws, regulations, or administrative provisions relating to the protection of animals used for experimental or other scientific purposes.

For each treatment, two male and two female cynomolgus monkeys received compound A or B (100 $\mu\text{g}/\text{animal}$ per day) or the vehicle (autologous serum) administered subcutaneously for 14 days. On day 15, all animals were humanely killed, and tissues for RNA extraction were immediately snap frozen and kept at -80°C until processing. Investigators were masked to treatment type.

RNA Expression Profiling

Total RNA was obtained from liver, kidney, spleen, thyroid gland, and pituitary by acid guanidinium isothiocyanate–phenol–chloroform extraction (12) using Trizol (Invitrogen Life Technologies, San Diego, CA, USA) and was purified on an affinity resin column (RNeasy; Qiagen, Hilden, Germany) according to the manufacturer's instructions. DNA microarray experiments were conducted as recommended by the manufacturer of the GeneChip system (Affymetrix Inc., Santa Clara, CA, USA) and as previously described (13). The human gene expression probe array used was HG-U95Av2 (Affymetrix), containing 12,627 probe sets interrogating approximately 10,000 full-length, annotated human genes. One GeneChip was used per tissue, per animal. The resultant image files (.dat files) were processed using the Microarray Analysis Suite 5 (MAS5) software (Affymetrix). Tab-delimited files containing data regarding signal intensity (Signal) and categorical expression level measurement (Absolute Call) were obtained. The data were quality checked and were transferred to GeneSpring software version 7.0 (Silicon Genetics, Redwood City, CA, USA) for analysis.

Data Analysis

Data were normalized by array to the 50th percentile of all measurements on that array, and each measurement for

each gene in those arrays was normalized to the mean of that gene's signal intensity measurements in the corresponding control arrays. To determine which genes were differentially expressed between the treatment groups (i.e., treated vs. nontreated), averages of gene expression levels in the groups were calculated; low values were cut off using a lower threshold of 20 [based on PM – MM calculation where the mismatch (MM) value is deducted from the perfect match (PM) value], and one-way analysis of variance (ANOVA) was applied to genes that had been marked *present* by Absolute Call (see above) in at least one of the samples of a given tissue. No multiple testing correction was applied. Genes with $p < 0.05$ were considered statistically significant. Group fold changes were calculated by using the mean of the signal intensities of the treatment group compared with the control group. Data were combined for the treated male and female animals and for the control groups.

To rank genes based on their ability to differentiate among multiple groups of conditions (e.g., tissues), the hypergeometric Fisher exact test (from *K*-nearest neighbors' class prediction tool) was applied. Specificity ranks were calculated by taking the inverse of the sum of the p value from ANOVA (nonspecific) and the inverse value of the class predictor Fisher exact test prediction strength ($1/\text{prediction strength}$). The final number was the rank of the gene's specificity to multiple groups [specificity rank = $1/(\text{ANOVA } p \text{ value} + 1/\text{prediction strength})$]. These filters can be applied to a dataset for individual tissues or can be used to identify genes with differential expression across tissues. The decision to keep or to reject a specific gene was based on the conjunction of numerical changes identified by comparative and statistical algorithms and on the relationship to other modulated genes that point to a common biologic theme. Data analysts assessed the weight of this relationship after a review of the relevant scientific literature. The annotation of the genes was determined by using NetAffx (<http://www.affymetrix.com/analysis/netaffix/index.affix>) (14). Information on probe sets was found in the literature or in the KEGG database (<http://www.genome.ad.jp/kegg/kegg2.html>).

RESULTS

At the end of the treatment period, more than 100 tissue samples per animal were dissected and snap frozen for storage. Total RNA was extracted from liver, kidney, spleen, thyroid gland, and pituitary and processed for gene expression profiling. Affymetrix microarray data were generated for each of the five tissue samples. The other stored tissues and organs may be evaluated if there was an indication from the analysis of the first five tissues that pointed to pathways better represented in specific tissues. The task of the investigators, who were masked to the treatment conditions, was to predict the identity or class of the peptide compounds with which the animals had been treated based solely on the gene expression signature from each compound.

To evaluate the effect of each compound on the transcriptome, genes were selected based on their expression level and on the statistical significance of the change in expression in all or a subset of the five tissues: kidney, liver, pituitary gland, spleen, and thyroid gland. This yielded a total

of 974 probe sets for compound A (ANOVA $p < 0.05$) and 1,074 probe sets for compound B (ANOVA $p < 0.01$).

Evaluation of Compound A

The bulk of changes in gene expression for compound A was related to signal transduction pathways through G-protein-coupled receptors (GPCRs) and glutamate receptors (Tables I and II). Downstream of these receptors, several pathways were affected, including the phosphatidylinositol 3'-kinase (PI3K), protein kinase C, phospholipase, calcium-calmodulin, Ras/mitogen-activated protein kinase/extracellular regulated kinase (Ras/MAPK/ERK), Janus kinase/signal transducer and activator of transcription (JAK/STAT), and adenylylate/guanylate cyclase pathways (Tables I and II). A large number of gene expression changes with compound A also involved factors governing cell growth and apoptosis (Table II). In particular, the growth hormone/insulin-like growth factor-1 (GH/IGF-1) and the glucagon/insulin axes were altered in several organs (Tables I and II). Growth factors such as growth hormone (GH) and IGF-1, or an upstream regulator of their secretion such as somatomedin, can elicit this type of response. However, the change in expression level of receptors suggested that compound A was most likely a ligand rather than a downstream effector.

The primary molecular evidence of an endocrine hormonal effect was derived from the pituitary findings, including the alteration of the glucagon/insulin axes (Table II). For example, the involvement of a GH-like effect in the pituitary was clearly suggested by the compound's impact on IGF1, the leptin receptor, and the prostaglandins (15–17). Therefore, the alteration of the subsequent following pathways, adenylylate cyclase, and phosphatidylinositol pointed to the transmission of the hormonal message through G-protein-coupled cell surface receptors (18–20). Other evidence, such as the effects on calcium, potassium channels, protein tyrosine phosphatases, and MAPKs, substantiated the hypothesis of the binding of a somatostatin receptor (SSTR) (21–25).

Based on these findings (i.e., signaling through G-protein-coupled receptors, effects on the entire GPCR downstream signaling cascade, changes in the GH/IGF-1 and insulin axes and on cell growth/apoptosis), we surmised that the effect of compound A was analogous to that of a somatomedin-like molecule (26). Binding to somatostatin receptors (SSTRs) results in activation of the PI3K signaling pathway, inhibition of adenylylate cyclase, activation of protein tyrosine phosphatases, modulation of MAPK, and coupling to inward-rectifying K^+ channels, voltage-dependent Ca^{2+} channels, Na^+/H^+ exchanger, AMPA/kainate glutamate

channels, phospholipase C, and phospholipase A_2 (27,28). Somatostatin receptor activation blocks cell secretion by inhibiting intracellular cyclic adenosine monophosphate and Ca^{2+} and by a receptor-linked distal effect on exocytosis. SSTR1, SSTR2, SSTR4, and SSTR5 induce cell cycle arrest through the phosphotyrosine phosphatase-dependent modulation of MAPK, associated with the induction of the retinoblastoma tumor-suppressor protein and p21. SSTR3 triggers phosphotyrosine phosphatase-dependent apoptosis accompanied by the activation of p53 and Bax. Deblinding revealed that compound A was the somatostatin analog SOM230 (Sandostatin[®]).

Evaluation of Compound B

Treatment with compound B demonstrated an expression profile that included numerous genes involved in the inflammatory cascade, from acute-phase protein generation to immune response and repair (Tables III and IV). This type of response can be elicited by many agents, such as lipopolysaccharide (LPS), interleukin-1 (IL-1), and some of the IL-6 family cytokines (29–31). On specific binding to their cellular receptors, the proinflammatory cytokines of the IL-6 family generate downstream signaling events that include the JAK/STAT pathway, the suppressor of cytokine signaling (SOCS), and the Ras/MAPK pathway responsible for the physical manifestations of inflammation, from amplification to repair. In this study, gp130, the signal transducing subunit of IL-6 family receptors [oncostatin M (OSM) receptor or IL-6 receptor], was observed to be strongly up-regulated in each organ (Tables III and IV).

To determine whether compound B was an LPS-like molecule or a proinflammatory cytokine, we looked for a gene expression signature of LPS. Lipopolysaccharide has been shown to bind to the cell surface molecule CD14, which acts as a signal enhancer and associates with toll-like receptor 4 (TLR4) (32,33). Toll-like receptors, which recognize pathogen-specific molecules by their extracellular leucine-rich repeat (LRR) domain, then activate a signaling cascade involving MyD88, IL-1 receptor-associated kinase, TRAF6, IKK α and β , JNK1, and NF- κ B through their cytoplasmic Toll/IL-1 receptor (TIR) domain and lead to the synthesis of inflammatory mediators, such as cytokines or nitric oxide. End products of this pathway are, for example, IL-1 and IL-6 family cytokines, such as OSM and leukemia inhibitory factor (LIF) (34–37). These factors can induce the expression of acute-phase proteins as an initial line of defense. None of the above-mentioned members of the Toll-receptor pathway were affected by treatment with compound

Table I. Data Analysts' Selection of Genes Deemed Most Significant in Guiding the Classification of Compound A

| Analysis | Results |
|-----------|---|
| Kidney | IGF2 ⁻ , SLC9A1, urocortin ⁺ , calmodulin 1 and 2 ⁺ , VEGF ⁺ , IGBP6 ⁻ , EIF ⁺ , CACNB1 ⁺ , DAXX ⁺ , histone ⁺ |
| Liver | IGF2 ⁻ , prostaglandin D2 synthase ⁺ , SLC9A1, calmodulin 1 and 2 ⁺ , VEGF ⁺ , EIF ⁺ , CACNB1 ⁺ , adenylylate cyclase 6 ⁺ , DAXX, histone ⁺ , leptin R ⁺ |
| Pituitary | prostaglandin D2 synthase ⁺ , calmodulin 1 and 2 ⁺ , VEGF ⁺ , EIF, adenylylate cyclase 6, histone ⁺ , leptin R ⁺ |
| Spleen | IGF2 ⁻ , prostaglandin D2 synthase ⁺ , calmodulin 1 and 2 ⁺ , VEGF ⁺ , IGBP6 ⁺ , CACNB1 ⁺ , adenylylate cyclase 6 ⁺ , DAXX ⁺ , histone ⁺ , leptin R |
| Thyroid | IGF2 ⁺ , IGBP6 ⁺ , EIF ⁺ , CACNB1 ⁺ , DAXX ⁺ , histone ⁺ |

+, Up-regulated expression in treated vs. nontreated animals; -, down-regulated expression in treated vs. nontreated animals.

Table II. Genes Affected by Treatment with Compound A

| Affymetrix ID | Gene title | Ratio of expression levels (treated/untreated) | | | | | Gene symbol | GenBank |
|--|--|--|-------|-----------------|--------|---------------|----------------|----------|
| | | Kidney | Liver | Pituitary gland | Spleen | Thyroid gland | | |
| <i>Adenylate/guanylate cyclases and related pathways</i> | | | | | | | | |
| 33134_at | Adenylate cyclase 3 | 1.3 | 1.3 | 1.4 | 1.2 | 1.4 | <i>ADCY3</i> | AB011083 |
| 39383_at | Adenylate cyclase 6 | 1.1 | 1.9 | 1.3 | 1.4 | 1.0 | <i>ADCY6</i> | AB007882 |
| 36754_at | Adenylate cyclase-activating polypeptide 1 (pituitary) | 0.8 | 0.6 | 0.9 | 0.8 | 0.7 | <i>ADCYAPI</i> | X60435 |
| 40788_at | Adenylate kinase 2 | 1.2 | 1.3 | 1.3 | 1.5 | 1.3 | <i>AK2</i> | U84371 |
| <i>Cell surface receptors</i> | | | | | | | | |
| 33470_at | Glutamate receptor-interacting protein 2 | 1.3 | 1.5 | 0.8 | 1.5 | 1.0 | <i>GRIP2</i> | AF052177 |
| 37134_f_at | Glutamate receptor, ionotropic, N-methyl-D-aspartate 1 | 1.0 | 2.6 | 1.4 | 1.4 | 1.4 | <i>GRIN1</i> | L13266 |
| 37135_f_at | Glutamate receptor, ionotropic, N-methyl-D-aspartate 1 | 1.0 | 5.4 | 1.9 | 1.9 | 0.7 | <i>GRIN1</i> | L13268 |
| 37308_at | G-protein-coupled receptor 107 | 1.3 | 1.4 | 1.6 | 1.3 | 1.1 | <i>GPR107</i> | AI888084 |
| 40299_at | G-protein-coupled receptor 161 | 1.4 | 1.5 | 1.2 | 1.5 | 0.9 | <i>GPR161</i> | AF091890 |
| 40300_g_at | G-protein-coupled receptor 161 | 1.5 | 1.6 | 1.0 | 1.1 | 1.0 | <i>GPR161</i> | AF091890 |
| 253_g_at | G-protein-coupled receptor 18 | 1.6 | 2.7 | 1.7 | 1.5 | 1.0 | <i>GPR18</i> | L42324 |
| 31700_at | G-protein-coupled receptor 35 | 1.3 | 1.1 | 1.1 | 1.3 | 0.9 | <i>GPR35</i> | AF027957 |
| 35769_at | G-protein-coupled receptor 56 | 1.4 | 1.1 | 1.2 | 1.1 | 1.2 | <i>GPR56</i> | AJ011001 |
| 1392_at | G-protein-coupled receptor kinase 6 | 1.6 | 1.7 | 1.2 | 1.2 | 0.8 | <i>GRK6</i> | L16862 |
| 40240_at | G-protein-coupled receptor, family C, group 5, member B | 1.3 | 1.0 | 1.6 | 1.5 | 1.5 | <i>GPRC5B</i> | AC004131 |
| 1457_at | Janus kinase 1 (a protein tyrosine kinase) | 0.9 | 1.5 | 1.2 | 2.1 | 1.0 | <i>JAK1</i> | M64174 |
| <i>Phosphatidylinositol and related pathways/PKC, phospholipases</i> | | | | | | | | |
| 33397_at | CDP-diacylglycerol-inositol 3-phosphatidyl transferase (phosphatidylinositol synthase) | 1.1 | 1.9 | 1.2 | 1.1 | 1.1 | <i>CDIPT</i> | AL050383 |
| 35755_at | Inositol 1,3,4-triphosphate 5/6 kinase | 1.5 | 1.2 | 2.3 | 1.4 | 1.3 | <i>ITPK1</i> | U51336 |
| 36154_at | Inositol hexaphosphate kinase 1 | 1.7 | 1.8 | 1.4 | 1.2 | 0.8 | <i>IHPK1</i> | D87452 |
| 656_at | Inositol polyphosphate-1-phosphatase | 1.8 | 1.4 | 1.7 | 1.6 | 1.2 | <i>INPPI</i> | L08488 |
| 41285_at | Inositol polyphosphate-5-phosphatase, 40 kDa | 1.8 | 2.4 | 0.9 | 2.2 | 1.0 | <i>INPP5A</i> | X77567 |
| 38960_at | Phosphatidylinositol (4,5) biphosphate 5-phosphatase, A | 1.3 | 0.9 | 1.2 | 1.6 | 1.3 | <i>PIB5PA</i> | U45975 |
| 37685_at | Phosphatidylinositol-binding clathrin assembly protein | 0.8 | 1.0 | 1.5 | 1.3 | 1.5 | <i>PICALM</i> | U45976 |
| 314_at | Phosphatidylinositol glycan, class B | 1.2 | 1.2 | 1.7 | 1.7 | 1.2 | <i>PIGB</i> | D42138 |
| 38297_at | Phosphatidylinositol transfer protein, membrane-associated 1 | 1.1 | 1.1 | 1.0 | 1.2 | 1.1 | <i>PITPNMI</i> | X98654 |
| 31833_at | Phosphatidylinositol-4-phosphate 5-kinase, type I, alpha | 1.1 | 3.0 | 1.8 | 2.2 | 1.4 | <i>PIP5K1A</i> | U78575 |
| 1269_at | Phosphoinositide-3-kinase, regulatory subunit, polypeptide 1 (p85 alpha) | 0.6 | 0.6 | 1.1 | 1.0 | 0.9 | <i>PIK3R1</i> | M61906 |
| 36151_at | Phospholipase D3 | 1.1 | 2.0 | 1.2 | 1.7 | 1.4 | <i>PLD3</i> | U60644 |
| 39711_at | Protein kinase C substrate 80K-H | 1.2 | 1.0 | 1.3 | 1.1 | 1.3 | <i>PRKCSH</i> | J03075 |
| 35853_at | Protein kinase C, alpha-binding protein | 1.5 | 1.1 | 1.0 | 1.3 | 1.5 | <i>PRKCABP</i> | AL049654 |
| <i>Protein tyrosine phosphatases/other phosphatases</i> | | | | | | | | |
| 922_at | Protein phosphatase 2 (formerly 2A), regulatory subunit A (PR 65), alpha isoform | 1.3 | 1.5 | 1.1 | 1.6 | 1.2 | <i>PPP2R1A</i> | J02902 |
| 1094_g_at | Protein phosphatase 2 (formerly 2A), regulatory subunit A (PR 65), beta isoform | 1.4 | 1.8 | 0.9 | 1.1 | 1.7 | <i>PPP2R1B</i> | M65254 |

Table II. Continued

| Affymetrix ID | Gene title | Ratio of expression levels (treated/untreated) | | | | | Gene symbol | GenBank |
|---|---|--|-------|-----------------|--------|---------------|----------------|----------|
| | | Kidney | Liver | Pituitary gland | Spleen | Thyroid gland | | |
| <i>Protein tyrosine phosphatases/other phosphatases</i> | | | | | | | | |
| 1383_at | Protein phosphatase 2 (formerly 2A), regulatory subunit B (PR 52), alpha isoform | 1.4 | 1.2 | 1.3 | 1.4 | 1.1 | <i>PPP2R2A</i> | M64929 |
| 903_at | Protein phosphatase 2, regulatory subunit B (B56), alpha isoform | 1.2 | 1.2 | 1.5 | 1.2 | 1.5 | <i>PPP2R5A</i> | L42373 |
| 39068_at | Protein phosphatase 2, regulatory subunit B (B56), delta isoform | 1.5 | 1.6 | 1.2 | 1.5 | 0.9 | <i>PPP2R5D</i> | L76702 |
| 39127_f_at | Protein phosphatase 2A, regulatory subunit B' (PR 53) | 1.3 | 1.7 | 1.5 | 1.6 | 1.6 | <i>PPP2R4</i> | X73478 |
| 38277_at | Protein phosphatase 3 (formerly 2B), catalytic subunit, beta isoform (calcineurin A beta) | 1.5 | 1.8 | 1.3 | 1.3 | 1.0 | <i>PPP3CB</i> | M29550 |
| 382_at | Protein phosphatase 4 (formerly X), catalytic subunit | 1.5 | 1.3 | 1.4 | 1.1 | 0.8 | <i>PPP4C</i> | X70218 |
| 392_g_at | Protein phosphatase 5, catalytic subunit | 1.9 | 1.4 | 1.3 | 1.6 | 0.8 | <i>PPP5C</i> | X89416 |
| 37581_at | Protein phosphatase 6, catalytic subunit | 1.1 | 1.4 | 1.4 | 2.0 | 1.6 | <i>PPP6C</i> | X92972 |
| 1241_at | Protein tyrosine phosphatase type IVA, member 2 | 1.3 | 0.9 | 1.3 | 1.1 | 1.3 | <i>PTP4A2</i> | U14603 |
| 36008_at | Protein tyrosine phosphatase type IVA, member 3 | 1.3 | 2.1 | 1.0 | 1.2 | 1.0 | <i>PTP4A3</i> | AF041434 |
| 588_at | Protein tyrosine phosphatase, nonreceptor type 1 | 1.8 | 1.4 | 2.1 | 2.1 | 1.3 | <i>PTPN1</i> | M31724 |
| 38443_at | Protein tyrosine phosphatase, nonreceptor type 11 (Noonan syndrome 1) | 1.3 | 1.1 | 1.6 | 1.3 | 0.9 | <i>PTPN11</i> | U79291 |
| 1463_at | Protein tyrosine phosphatase, nonreceptor type 12 | 1.1 | 1.1 | 1.6 | 1.7 | 1.1 | <i>PTPN12</i> | M93425 |
| 34198_at | Protein tyrosine phosphatase, nonreceptor type 13 (APO-1/CD95 (Fas)-associated phosphatase) | 0.8 | 0.1 | 0.9 | 1.0 | 1.2 | <i>PTPN13</i> | U12128 |
| 41782_g_at | Protein tyrosine phosphatase, receptor type, F polypeptide (PTPRF), interacting protein (liprin), alpha 1 | 1.9 | 1.4 | 1.5 | 1.6 | 0.9 | <i>PPFIA1</i> | U22815 |
| <i>Ras/MAPK/ERK-related pathways and adaptor proteins</i> | | | | | | | | |
| 36660_at | RAB11A, member RAS oncogene family | 1.2 | 1.7 | 0.9 | 1.5 | 1.9 | <i>RAB11A</i> | AF000231 |
| 40210_at | RAB13, member RAS oncogene family | 1.3 | 3.0 | 4.9 | 1.2 | 1.5 | <i>RAB13</i> | X75593 |
| 35325_at | RAB14, member RAS oncogene family | 1.4 | 0.9 | 1.4 | 1.2 | 1.3 | <i>RAB14</i> | AF052113 |
| 1074_at | RAB1A, member RAS oncogene family | 1.3 | 1.2 | 1.5 | 1.9 | 1.0 | <i>RAB1A</i> | M28209 |
| 623_s_at | RAB2, member RAS oncogene family | 1.1 | 1.3 | 1.3 | 1.2 | 1.1 | <i>RAB2</i> | M28213 |
| 39272_g_at | RAB4B, member RAS oncogene family | 1.0 | 1.4 | 1.3 | 1.6 | 1.6 | <i>RAB4B</i> | AA461365 |
| 37362_at | RAB5B, member RAS oncogene family | 1.1 | 1.5 | 1.4 | 1.5 | 1.1 | <i>RAB5B</i> | X54871 |
| 35304_at | RAB6A, member RAS oncogene family | 0.9 | 1.3 | 1.2 | 1.7 | 1.1 | <i>RAB6A</i> | AF052130 |
| 35339_at | RAB8A, member RAS oncogene family | 1.3 | 0.9 | 1.1 | 1.6 | 1.0 | <i>RAB8A</i> | AI743606 |
| 39628_at | RAB9A, member RAS oncogene family | 1.1 | 1.0 | 1.2 | 1.2 | 1.3 | <i>RAB9A</i> | AI671547 |

Table II. Continued

| Affymetrix ID | Gene title | Ratio of expression levels (treated/untreated) | | | | | Gene symbol | GenBank |
|---|--|--|-------|-----------------|--------|---------------|-----------------|----------|
| | | Kidney | Liver | Pituitary gland | Spleen | Thyroid gland | | |
| <i>Ras/MAPK/ERK-related pathways and adaptor proteins</i> | | | | | | | | |
| 1394_at | Ras homolog gene family, member A | 1.3 | 1.1 | 1.5 | 1.3 | 1.6 | <i>RHOA</i> | L25080 |
| 1395_at | Ras homolog gene family, member C | 1.5 | 1.6 | 1.3 | 1.5 | 1.3 | <i>RHOC</i> | L25081 |
| 31846_at | Ras homolog gene family, member D | 1.0 | 1.5 | 1.8 | 2.2 | 1.2 | <i>RHOD</i> | AW003733 |
| 36902_at | Ras homolog gene family, member G (rho G) | 1.4 | 1.3 | 1.2 | 1.2 | 1.0 | <i>RHOG</i> | X61587 |
| 1675_at | RAS p21 protein activator (GTPase-activating protein) 1 | 1.0 | 1.2 | 1.5 | 1.7 | 1.0 | <i>RASAI</i> | M23379 |
| 40864_at | Ras-related C3 botulinum toxin substrate 1 (rho family, small GTP-binding protein Rac1) | 1.2 | 1.3 | 1.7 | 1.5 | 1.0 | <i>RAC1</i> | D25274 |
| 39989_at | Ras-related GTP binding B | 2.2 | 1.9 | 1.2 | 1.5 | 1.9 | <i>RRAGB</i> | X90530 |
| 1000_at | Mitogen-activated protein kinase 3 | 1.5 | 1.0 | 1.2 | 1.3 | 1.1 | <i>MAPK3</i> | X60188 |
| 35617_at | Mitogen-activated protein kinase 7 | 1.0 | 1.6 | 1.6 | 1.4 | 1.2 | <i>MAPK7</i> | U29725 |
| 41279_f_at | Mitogen-activated protein kinase 8 interacting protein 1 | 1.5 | 1.4 | 1.3 | 1.2 | 1.1 | <i>MAPK8IP1</i> | AF007134 |
| 1238_at | Mitogen-activated protein kinase 9 | 1.4 | 1.2 | 1.7 | 1.1 | 1.4 | <i>MAPK9</i> | U09759 |
| 1844_s_at | Mitogen-activated protein kinase kinase 1 | 1.5 | 1.8 | 1.2 | 1.7 | 0.8 | <i>MAP2K1</i> | L05624 |
| 1398_g_at | Mitogen-activated protein kinase kinase kinase 11 | 1.3 | 1.3 | 2.0 | 1.5 | 1.0 | <i>MAP3K11</i> | L32976 |
| 520_at | Mitogen-activated protein kinase kinase kinase 12 | 1.2 | 1.3 | 0.9 | 1.9 | 1.1 | <i>MAP3K12</i> | U07358 |
| 35651_at | Mitogen-activated protein kinase kinase kinase 4 | 1.0 | 1.4 | 1.6 | 1.4 | 1.2 | <i>MAP3K4</i> | AF002715 |
| 1327_s_at | Mitogen-activated protein kinase kinase kinase 5 | 1.5 | 1.1 | 1.2 | 1.6 | 1.4 | <i>MAP3K5</i> | U67156 |
| 36179_at | Mitogen-activated protein kinase-activated protein kinase 2 | 1.4 | 1.6 | 1.5 | 1.2 | 1.2 | <i>MAPKAPK2</i> | U12779 |
| <i>GH/IGF/glucagon/insulin axis</i> | | | | | | | | |
| 36782_s_at | Insulin-like growth factor 2 (somatomedin A) | 0.5 | 0.5 | 1.0 | 0.3 | 1.3 | <i>IGF2</i> | J03242 |
| 1741_s_at | Insulin-like growth factor binding protein 2, 36 kDa | 1.8 | 2.1 | 2.0 | 2.0 | 1.2 | <i>IGFBP2</i> | S37730 |
| 37319_at | Insulin-like growth factor binding protein 3 | 1.1 | 1.0 | 1.7 | 1.4 | 1.2 | <i>IGFBP3</i> | M35878 |
| 39781_at | Insulin-like growth factor binding protein 4 | 0.9 | 1.2 | 1.5 | 1.3 | 1.4 | <i>IGFBP4</i> | U20982 |
| 1736_at | Insulin-like growth factor binding protein 6 | 1.4 | 1.0 | 1.1 | 1.8 | 2.0 | <i>IGFBP6</i> | M62402 |
| 41752_at | Growth hormone-inducible transmembrane protein | 1.0 | 1.6 | 1.5 | 1.6 | 1.7 | <i>GHITM</i> | W28190 |
| 33830_at | Leptin receptor | 1.0 | 1.5 | 1.4 | 1.3 | 1.2 | <i>LEPR</i> | AW026535 |
| 38406_f_at | Prostaglandin D2 synthase 21 kDa (brain) | 1.2 | 1.9 | 1.3 | 3.8 | 1.0 | <i>PTGDS</i> | AI207842 |
| 33772_at | Prostaglandin E receptor 4 (subtype EP4) | 0.8 | 0.6 | 0.4 | 1.2 | 0.5 | <i>PTGER4</i> | L25124 |
| 41246_at | Serine (or cysteine) proteinase inhibitor, clade E (nexin, plasminogen activator inhibitor type 1), member 2 | 1.2 | 1.2 | 2.5 | 1.0 | 1.3 | <i>SERPINE2</i> | AI743134 |
| <i>Ion channels and related pathways</i> | | | | | | | | |
| 38516_at | Sodium channel, voltage-gated, type I, beta | 1.6 | 1.3 | 1.4 | 1.1 | 1.2 | <i>SCN1B</i> | L10338 |
| 36558_at | Calcium channel, voltage-dependent, beta 1 subunit | 1.0 | 1.3 | 1.1 | 1.9 | 1.4 | <i>CACNB1</i> | M92302 |
| 38225_at | Potassium voltage-gated channel, subfamily H (eag-related), member 2 | 1.1 | 0.6 | 0.7 | 0.4 | 0.9 | <i>KCNH2</i> | AF052728 |

Table II. Continued

| Affymetrix ID | Gene title | Ratio of expression levels (treated/untreated) | | | | | Gene symbol | GenBank |
|--|--|--|-------|-----------------|--------|---------------|---------------|----------|
| | | Kidney | Liver | Pituitary gland | Spleen | Thyroid gland | | |
| <i>Ion channels and related pathways</i> | | | | | | | | |
| 40527_at | Potassium voltage-gated channel, KQT-like subfamily, member 1 | 1.2 | 1.7 | 1.4 | 1.4 | 1.5 | <i>KCNQ1</i> | AF000571 |
| 31608_g_at | Voltage-dependent anion channel 1 | 1.5 | 1.7 | 1.4 | 1.5 | 1.2 | <i>VDAC1</i> | AJ002428 |
| 37697_s_at | Voltage-dependent anion channel 2 | 1.0 | 1.2 | 1.9 | 1.4 | 1.8 | <i>VDAC2</i> | L08666 |
| 36102_at | Voltage-dependent anion channel 3 | 1.3 | 1.2 | 1.6 | 1.3 | 1.4 | <i>VDAC3</i> | AF038962 |
| 38225_at | Potassium voltage-gated channel, subfamily H (eag-related), member 2 | 1.1 | 0.6 | 0.7 | 0.4 | 0.9 | <i>KCNH2</i> | AF052728 |
| <i>Cell growth/proliferation</i> | | | | | | | | |
| 39388_at | Calcium/calmodulin-dependent protein kinase (CaM kinase) II gamma | 1.7 | 1.5 | 1.7 | 1.7 | 1.1 | <i>CAMK2G</i> | AA902713 |
| 251_at | Calcium/calmodulin-dependent protein kinase I | 1.7 | 2.0 | 1.4 | 1.3 | 1.0 | <i>CAMK1</i> | L41816 |
| 33514_at | Calcium/calmodulin-dependent protein kinase IV | 0.6 | 0.3 | 0.5 | 1.1 | 0.3 | <i>CAMK4</i> | D30742 |
| 38716_at | Calcium/calmodulin-dependent protein kinase kinase 2, beta | 1.7 | 2.7 | 1.8 | 1.7 | 1.0 | <i>CAMKK2</i> | AB018330 |
| 41739_s_at | Caldesmon 1 | 1.3 | 1.0 | 1.6 | 1.7 | 1.2 | <i>CALD1</i> | M83216 |
| 41288_at | Calmodulin 1 (phosphorylase kinase, delta) | 1.1 | 1.4 | 1.5 | 1.1 | 1.9 | <i>CALM1</i> | AL036744 |
| 33458_r_at | Calmodulin 2 (phosphorylase kinase, delta) | 0.8 | 1.4 | 1.6 | 1.9 | 1.4 | <i>CALM2</i> | AI688098 |
| 41421_at | Calmodulin-binding transcription activator 2 | 1.2 | 1.1 | 1.5 | 1.3 | 1.2 | <i>CAMTA2</i> | AB020716 |
| 40887_g_at | Eukaryotic translation elongation factor 1 alpha 1 | 1.3 | 2.1 | 1.7 | 1.6 | 1.3 | <i>EEF1A1</i> | L41498 |
| 41256_at | Eukaryotic translation elongation factor 1 delta (guanine nucleotide exchange protein) | 1.3 | 1.5 | 1.8 | 1.3 | 1.4 | <i>EEF1D</i> | Z21507 |
| 40587_s_at | Eukaryotic translation elongation factor 1 epsilon 1 | 1.1 | 1.2 | 1.3 | 1.3 | 1.4 | <i>EEF1E1</i> | AF054186 |
| 36587_at | Eukaryotic translation elongation factor 2 | 1.2 | 1.0 | 1.2 | 1.0 | 1.2 | <i>EEF2</i> | Z11692 |
| 1154_at | Eukaryotic translation initiation factor 2, subunit 1 alpha, 35 kDa | 1.3 | 1.4 | 1.1 | 1.2 | 1.1 | <i>EIF2S1</i> | J02645 |
| 39368_at | Eukaryotic translation initiation factor 2, subunit 2 beta, 38 kDa | 1.1 | 1.2 | 1.4 | 1.3 | 1.2 | <i>EIF2S2</i> | AL031668 |
| 1272_at | Eukaryotic translation initiation factor 2, subunit 3 gamma, 52 kDa | 1.7 | 1.8 | 1.1 | 2.1 | 1.4 | <i>EIF2S3</i> | L19161 |
| 40515_at | Eukaryotic translation initiation factor 2B, subunit 2 beta, 39 kDa | 1.3 | 1.4 | 1.0 | 1.5 | 1.0 | <i>EIF2B2</i> | AF035280 |
| 32659_at | Eukaryotic translation initiation factor 2B, subunit 4 delta, 67 kDa | 1.3 | 1.5 | 1.2 | 1.3 | 1.1 | <i>EIF2B4</i> | AL050109 |
| 34758_at | Eukaryotic translation initiation factor 2B, subunit 5 epsilon, 82 kDa | 1.5 | 1.7 | 1.1 | 1.4 | 1.3 | <i>EIF2B5</i> | U23028 |
| 1644_at | Eukaryotic translation initiation factor 3, subunit 2 beta, 36 kDa | 2.1 | 1.9 | 1.2 | 1.6 | 1.8 | <i>EIF3S2</i> | U36764 |
| 35298_at | Eukaryotic translation initiation factor 3, subunit 7 zeta, 66/67 kDa | 1.6 | 1.5 | 1.2 | 1.3 | 1.6 | <i>EIF3S7</i> | U54558 |
| 32844_at | Eukaryotic translation initiation factor 4 gamma, 1 | 1.4 | 1.4 | 1.1 | 1.2 | 1.5 | <i>EIF4G1</i> | AF104913 |
| 41785_at | Eukaryotic translation initiation factor 4 gamma, 2 | 1.1 | 1.3 | 1.6 | 1.3 | 1.1 | <i>EIF4G2</i> | U73824 |
| 1199_at | Eukaryotic translation initiation factor 4A, isoform 1 | 1.3 | 1.7 | 1.2 | 1.4 | 1.0 | <i>EIF4A1</i> | D13748 |
| 1420_s_at | Eukaryotic translation initiation factor 4A, isoform 2 | 1.3 | 1.4 | 1.4 | 1.4 | 1.2 | <i>EIF4A2</i> | D30655 |

Table II. Continued

| Affymetrix ID | Gene title | Ratio of expression levels (treated/untreated) | | | | | Gene symbol | GenBank |
|----------------------------------|--|--|-------|-----------------|--------|---------------|------------------|----------|
| | | Kidney | Liver | Pituitary gland | Spleen | Thyroid gland | | |
| <i>Cell growth/proliferation</i> | | | | | | | | |
| 39110_at | Eukaryotic translation initiation factor 4B | 1.3 | 2.7 | 1.4 | 2.4 | 2.2 | <i>EIF4B</i> | X55733 |
| 31597_r_at | Eukaryotic translation initiation factor 4E binding protein 1 | 2.1 | 1.8 | 0.9 | 3.3 | 1.1 | <i>EIF4EBP1</i> | L36055 |
| 32229_at | Eukaryotic translation initiation factor 4E-like 3 | 1.2 | 1.9 | 1.1 | 1.2 | 1.4 | <i>EIF4EL3</i> | AF038957 |
| 40537_at | Eukaryotic translation initiation factor 5B | 1.1 | 0.9 | 1.1 | 1.3 | 1.3 | <i>EIF5B</i> | AB018284 |
| 37318_at | Eukaryotic translation termination factor 1 | 1.5 | 1.1 | 1.1 | 1.1 | 1.2 | <i>ETF1</i> | X81625 |
| 38418_at | Cyclin D1 (PRAD1: parathyroid adenomatosis 1) | 1.3 | 1.2 | 1.1 | 1.3 | 1.3 | <i>CCND1</i> | X59798 |
| 41060_at | Cyclin E1 | 1.9 | 0.9 | 1.6 | 1.0 | 1.5 | <i>CCNE1</i> | M74093 |
| 1836_at | Cyclin I | 0.7 | 0.8 | 0.7 | 0.5 | 0.8 | <i>CCNI</i> | D50310 |
| 39417_at | Cyclin-dependent kinase (CDC2-like) 11 | 1.4 | 1.4 | 3.2 | 1.2 | 1.5 | <i>CDK11</i> | AB028951 |
| 1792_g_at | Cyclin-dependent kinase 2 | 1.2 | 1.2 | 1.1 | 1.3 | 1.1 | <i>CDK2</i> | M68520 |
| 1942_s_at | Cyclin-dependent kinase 4 | 1.1 | 1.3 | 1.1 | 1.3 | 1.4 | <i>CDK4</i> | U37022 |
| 40549_at | Cyclin-dependent kinase 5 | 2.3 | 1.8 | 1.2 | 3.5 | 1.9 | <i>CDK5</i> | L04658 |
| 799_at | Cyclin-dependent kinase 5, regulatory subunit 1 (p35) | 1.3 | 1.6 | 0.9 | 1.3 | 1.2 | <i>CDK5R1</i> | X80343 |
| 795_s_at | Cyclin-dependent kinase-like 1 (CDC2-related kinase) | 1.6 | 2.0 | 1.5 | 2.6 | 1.0 | <i>CDKLI</i> | X66358 |
| 40404_s_at | CDC16 cell division cycle 16 homolog (<i>Saccharomyces cerevisiae</i>) | 1.3 | 1.3 | 1.7 | 1.4 | 1.2 | <i>CDC16</i> | U18291 |
| 505_at | CDC37 cell division cycle 37 homolog (<i>S. cerevisiae</i>) | 1.7 | 1.4 | 1.4 | 1.8 | 1.2 | <i>CDC37</i> | U43077 |
| 1005_at | Dual-specificity phosphatase 1 | 2.4 | 1.6 | 1.6 | 2.6 | 1.0 | <i>DUSP1</i> | X68277 |
| 1597_at | Growth arrest-specific 6 | 1.8 | 4.6 | 1.6 | 1.8 | 1.0 | <i>GAS6</i> | L13720 |
| 887_at | Growth differentiation factor 1 | 1.9 | 1.4 | 1.1 | 1.8 | 0.8 | <i>GDF1</i> | M62302 |
| 1890_at | Growth differentiation factor 15 | 1.5 | 1.6 | 0.9 | 1.4 | 2.0 | <i>GDF15</i> | AB000584 |
| 1680_at | Growth factor receptor-bound protein 7 | 1.7 | 2.1 | 1.3 | 1.5 | 0.8 | <i>GRB7</i> | D43772 |
| 34308_at | Histone 1, H2AC | 1.1 | 1.6 | 0.9 | 1.2 | 1.1 | <i>HIST1H2AC</i> | U90551 |
| 34157_f_at | Histone 1, H2AL | 1.6 | 2.1 | 1.7 | 1.8 | 1.4 | <i>HIST1H2AL</i> | AI200373 |
| 31523_f_at | Histone 1, H2BE | 1.7 | 1.3 | 1.1 | 1.9 | 1.7 | <i>HIST1H2BE</i> | Z80780 |
| 31528_f_at | Histone 1, H2BM | 2.7 | 1.5 | 1.2 | 2.4 | 1.4 | <i>HIST1H2BM</i> | Z83738 |
| 36347_f_at | Histone 1, H2BN | 1.8 | 1.2 | 1.4 | 1.5 | 1.6 | <i>HIST1H2BN</i> | AA873858 |
| 762_f_at | Histone 1, H4I | 1.6 | 2.2 | 1.2 | 1.3 | 2.0 | <i>HIST1H4I</i> | AB000905 |
| 31521_f_at | Histone 1, H4J | 1.2 | 1.8 | 1.2 | 1.6 | 2.8 | <i>HIST1H4J</i> | X60484 |
| 286_at | Histone 2, H2AA | 1.5 | 1.2 | 1.3 | 1.2 | 1.8 | <i>HIST2H2AA</i> | L19779 |
| 476_s_at | Histone deacetylase 1 | 1.7 | 1.9 | 1.2 | 2.8 | 0.8 | <i>HDAC1</i> | U50079 |
| 38810_at | Histone deacetylase 5 | 1.2 | 1.5 | 1.3 | 1.2 | 1.0 | <i>HDAC5</i> | AF039241 |
| 1470_at | Polymerase (DNA directed), delta 2, regulatory subunit 50 kDa | 1.1 | 1.1 | 1.7 | 0.9 | 1.6 | <i>POLD2</i> | U21090 |
| 38397_at | Polymerase (DNA-directed), delta 4 | 1.3 | 1.4 | 1.9 | 1.1 | 1.2 | <i>POLD4</i> | U09196 |
| 1594_at | Polymerase (RNA) II (DNA directed) polypeptide C, 33 kDa | 1.1 | 1.3 | 1.1 | 1.0 | 1.6 | <i>POLR2C</i> | J05448 |
| 39747_at | Polymerase (RNA) II (DNA directed) polypeptide G | 1.5 | 1.2 | 0.9 | 1.3 | 1.3 | <i>POLR2G</i> | U52427 |
| 1248_at | Polymerase (RNA) II (DNA directed) polypeptide H | 1.5 | 1.2 | 1.4 | 1.2 | 1.0 | <i>POLR2H</i> | U37689 |
| 1486_at | Polymerase (RNA) II (DNA directed) polypeptide J, 13.3 kDa | 1.5 | 1.7 | 1.5 | 1.6 | 1.5 | <i>POLR2J</i> | L37127 |
| 35841_at | Polymerase (RNA) II (DNA directed) polypeptide L, 7.6 kDa | 1.2 | 1.2 | 1.1 | 1.1 | 1.2 | <i>POLR2L</i> | N24355 |
| 782_at | Polymerase (RNA) III (DNA directed) polypeptide C (62 kDa) | 1.5 | 0.9 | 1.0 | 1.2 | 1.8 | <i>POLR3C</i> | U93867 |
| 34320_at | Polymerase I and transcript release factor | 1.4 | 1.6 | 1.5 | 1.5 | 1.9 | <i>PTRF</i> | AL050224 |

Table II. Continued

| Affymetrix ID | Gene title | Ratio of expression levels (treated/untreated) | | | | | Gene symbol | GenBank |
|----------------------------------|---|--|-------|-----------------|--------|---------------|-----------------|----------|
| | | Kidney | Liver | Pituitary gland | Spleen | Thyroid gland | | |
| <i>Cell growth/proliferation</i> | | | | | | | | |
| 2010_at | S-phase kinase-associated protein 1A (p19a) | 1.3 | 1.8 | 1.5 | 1.8 | 1.4 | <i>SKPIA</i> | U33760 |
| 1685_at | S-phase response (cyclin related) | 0.9 | 1.1 | 1.8 | 1.9 | 0.8 | <i>SPHAR</i> | X82554 |
| <i>Apoptosis</i> | | | | | | | | |
| 36199_at | Death-associated protein | 1.5 | 0.9 | 0.9 | 1.0 | 2.3 | | X76105 |
| 1754_at | Death-associated protein 6 | 1.4 | 2.6 | 1.2 | 1.9 | 1.1 | | AF006041 |
| 822_s_at | CASP2 and RIPK1 domain containing adaptor with death domain | 1.7 | 1.4 | 1.1 | 1.7 | 1.2 | | U79115 |
| 1326_at | Caspase 10, apoptosis-related cysteine protease | 0.9 | 0.9 | 0.8 | 0.9 | 0.7 | <i>CASP10</i> | U60519 |
| 486_at | Caspase 9, apoptosis-related cysteine protease | 1.3 | 1.7 | 1.4 | 2.4 | 1.0 | <i>CASP9</i> | U60521 |
| 41816_at | Caspase recruitment domain family, member 10 | 1.4 | 1.3 | 2.0 | 2.6 | 0.7 | <i>CARD10</i> | AL049851 |
| 1861_at | BCL2-antagonist of cell death | 1.3 | 1.1 | 1.3 | 1.5 | 1.1 | <i>BAD</i> | U66879 |
| 38050_at | BCL2-associated transcription factor 1 | 1.3 | 1.1 | 2.1 | 1.8 | 0.8 | <i>BCLAF1</i> | D79986 |
| 2067_f_at | BCL2-associated X protein | 1.2 | 2.0 | 1.2 | 2.0 | 1.8 | <i>BAX</i> | L22475 |
| 1615_at | BCL2-like 1 | 1.2 | 1.1 | 1.3 | 1.6 | 0.9 | <i>BCL2L1</i> | Z23115 |
| 36211_at | BCL2-like 2 | 1.4 | 1.4 | 1.2 | 1.4 | 1.1 | <i>BCL2L2</i> | D87461 |
| 609_f_at | Metallothionein 1B (functional) | 1.1 | 1.1 | 1.6 | 1.4 | 1.9 | <i>MTIB</i> | M13485 |
| 36130_f_at | Metallothionein 1E (functional) | 1.0 | 0.7 | 2.0 | 1.7 | 2.1 | <i>MTIE</i> | R92331 |
| 41446_f_at | Metallothionein 1F (functional) | 1.0 | 1.3 | 1.6 | 1.3 | 2.1 | <i>MTIF</i> | H68340 |
| 39594_f_at | Metallothionein 1H | 1.2 | 1.1 | 1.3 | 1.2 | 2.1 | <i>MTIH</i> | R93527 |
| 855_at | Programmed cell death 2 | 1.3 | 0.9 | 1.7 | 0.9 | 1.2 | <i>PDCD2</i> | S78085 |
| 37569_at | Programmed cell death 6 | 1.1 | 1.1 | 1.4 | 1.3 | 1.2 | <i>PDCD6</i> | AF035606 |
| 32212_at | Programmed cell death 8 (apoptosis-inducing factor) | 1.1 | 1.3 | 1.1 | 1.6 | 1.4 | <i>PDCD8</i> | AL049703 |
| 1715_at | Tumor necrosis factor (ligand) superfamily, member 10 | 1.0 | 1.5 | 3.0 | 0.9 | 1.3 | <i>TNFSF10</i> | U37518 |
| 1563_s_at | Tumor necrosis factor receptor superfamily, member 1A | 1.2 | 1.3 | 1.2 | 1.8 | 1.2 | <i>TNFRSF1A</i> | M58286 |

B. We concluded that the gene expression signature was not strongly related to the LPS signaling cascade.

We also considered whether a tumor necrosis factor (TNF)-like molecule may be compound B. Binding of TNF to one of its receptors can lead to induction of apoptosis

through the involvement of death domain containing TNF-receptor binding proteins like TNF-receptor-associated death domain (TRADD) or Fas-associated death domain (FADD) or to the activation of NF- κ B through I κ B kinase (38,39). None of the TNF-receptor associated proteins were affected

Table III. Data Analysts' Selection of Genes Deemed Most Significant in Guiding the Classification of Compound B

| Analysis | Results |
|-----------|--|
| Kidney | C/EBP delta ⁺ , JunB ⁺ , gp130 ⁺ , STAT3 ⁺ , SOCS2 ⁺ , TIMP-1 ⁺⁺ , VCAM ⁺ , osteopontin ⁺ , collagen ⁺ , annexin A3 ⁺ , CD83 ⁻ , CCL2 ⁺ , FGF1 ⁻ , haptoglobin ⁺ , caspase 4 ⁺ , serpinA3 ⁺ , selectin P ⁺ , phospholipase AII type II ⁺ |
| Liver | C/EBP delta ⁺ , JunB ⁺ , gp130 ⁺ , STAT3 ⁺ , SOCS2 ⁺ , TIMP-1 ⁺⁺⁺ , osteopontin ⁺ , collagen ⁺ , caspase 4 ⁺ , annexin A3 ⁺ , CD83 ⁻ , CCL2 ⁺ , FGF1 ⁻ , serpinA3 ⁺ , selectin P ⁺ , phospholipase AII type II ⁺ , VCAM ⁺ |
| Pituitary | C/EBP delta ⁺ , JunB ⁺ , gp130 ⁺ , STAT3 ⁺ , SOCS2 ⁺ , TIMP-1, VCAM ⁺⁺ , osteopontin ⁺ , collagen ⁺ , caspase 4 ⁺ , annexin A3 ⁺ , CD83 ⁻ , FGF1 ⁻ , haptoglobin ⁺ , serpinA3 ⁺ , selectin P ⁺ |
| Spleen | C/EBP delta ⁺ , JunB ⁺ , gp130 ⁺ , STAT 3 ⁺ , SOCS2 ⁺ , TIMP-1 ⁺ , collagen ⁺ , caspase 4 ⁺ , CD83 ⁻ , FGF1 ⁻ , haptoglobin ⁺ , serpinA3 ⁺ , phospholipase AII type II ⁺ |
| Thyroid | C/EBP delta ⁺ , JunB ⁺ , gp130 ⁺ , STAT3 ⁺ , SOCS2 ⁺ , TIMP-1 ⁺ , VCAM ⁺ , osteopontin ⁺ , collagen ⁺ , caspase 4 ⁺ , annexin A3 ⁺ , CD83 ⁻ , CCL2 ⁺ , FGF1 ⁻ , haptoglobin ⁺ , serpinA3 ⁺ , selectin P ⁺ , phospholipase AII type II ⁺ |

+, Up-regulated expression in treated vs. nontreated animals; -, down-regulated expression in treated vs. nontreated animals.

Table IV. Genes Affected by Treatment with Compound B

| Affymetrix ID | Gene title | Ratio of expression levels (treated/untreated) | | | | | Gene symbol | GenBank |
|-----------------------------|--|--|-------|-----------------|--------|---------------|-----------------|----------|
| | | Kidney | Liver | Pituitary gland | Spleen | Thyroid gland | | |
| <i>Acute-phase response</i> | | | | | | | | |
| 36780_at | Clusterin (complement lysis inhibitor, SP-40,40, sulfated glycoprotein 2, testosterone-repressed prostate message 2, apolipoprotein J) | 1.9 | 1.2 | 1.7 | 3.4 | 2.7 | <i>CLU</i> | M25915 |
| 38052_at | Coagulation factor XIII, A1 polypeptide | 1.1 | 1.4 | 1.6 | 1.9 | 1.2 | <i>FI3AI</i> | M14539 |
| 40766_at | Complement component 4A | 3.7 | 1.2 | 2.1 | 1.3 | 3.5 | <i>C4A</i> | U24578 |
| 31444_s_at | Annexin A2 | 1.5 | 1.5 | 1.5 | 1.6 | 2.3 | <i>ANXA2</i> | M62895 |
| 31792_at | Annexin A3 | 3.2 | 5.2 | 1.7 | 1.2 | 2.1 | <i>ANXA3</i> | M20560 |
| 428_s_at | Beta-2-microglobulin | 1.3 | 1.1 | 1.4 | 1.2 | 1.4 | <i>B2M</i> | V00567 |
| 32550_r_at | CCAAT/enhancer-binding protein (C/EBP), alpha | 0.8 | 0.5 | 0.7 | 0.9 | 0.8 | <i>CEBPA</i> | Y11525 |
| 38354_at | CCAAT/enhancer-binding protein (C/EBP), beta | 2.2 | 0.8 | 2.5 | 1.9 | 1.2 | <i>CEBPB</i> | X52560 |
| 1052_s_at | CCAAT/enhancer-binding protein (C/EBP), delta | 3.6 | 2.8 | 3.6 | 2.2 | 3.0 | <i>CEBPD</i> | M83667 |
| 229_at | CCAAT/enhancer-binding protein zeta | 1.2 | 1.2 | 1.1 | 1.3 | 2.1 | <i>CEBPZ</i> | M37197 |
| 39008_at | Ceruloplasmin (ferroxidase) | 1.2 | 1.6 | 5.0 | 1.6 | 1.4 | <i>CP</i> | M13699 |
| 32363_at | Cholesterol 25-hydroxylase | 3.2 | 3.6 | 2.1 | 2.3 | 2.1 | <i>CH25H</i> | AF059214 |
| 38111_at | Chondroitin sulfate proteoglycan 2 (versican) | 1.8 | 3.7 | 5.5 | 2.0 | 1.1 | <i>CSPG2</i> | X15998 |
| 36984_f_at | Haptoglobin | 2.2 | 1.2 | 3.4 | 1.8 | 2.8 | <i>HP</i> | X89214 |
| 37621_at | Interleukin-6 signal transducer (gp130, oncostatin M receptor) | 1.5 | 1.5 | 1.2 | 2.3 | 1.4 | <i>IL6ST</i> | M57230 |
| 2049_s_at | Jun B proto-oncogene | 4.7 | 8.6 | 1.8 | 3.8 | 5.5 | <i>JUNB</i> | M29039 |
| 37025_at | Lipopolysaccharide-induced tumor necrosis factor | 2.7 | 2.1 | 1.6 | 1.6 | 2.1 | <i>LITAF</i> | AL120815 |
| 32855_at | Low-density lipoprotein receptor (familial hypercholesterolemia) | 6.7 | 2.3 | 12.9 | 4.7 | 2.5 | <i>LDLR</i> | L00352 |
| 39428_at | Lymphocyte adaptor protein | 1.8 | 1.9 | 1.7 | 1.3 | 1.4 | <i>LNK</i> | AF055581 |
| 1497_at | Lymphotoxin beta receptor (tumor necrosis factor receptor superfamily, member 3) | 2.0 | 1.2 | 1.6 | 3.6 | 2.3 | <i>LTBR</i> | L04270 |
| 1648_at | Oncostatin M receptor | 1.8 | 4.6 | 2.6 | 1.6 | 3.7 | <i>OSMR</i> | U60805 |
| 614_at | Phospholipase A2, group IIA (platelets, synovial fluid) | 2.0 | 10.4 | 1.1 | 2.0 | 8.5 | <i>PLA2G2A</i> | M22430 |
| 32569_at | Platelet-activating factor acetylhydrolase, isoform Ib, alpha subunit 45 kDa | 0.9 | 0.7 | 0.7 | 0.9 | 0.6 | <i>PAFAH1B1</i> | L13385 |
| 32691_s_at | Prostaglandin E receptor 3 (subtype EP3) | 1.0 | 1.4 | 1.1 | 1.1 | 1.7 | <i>PTGER3</i> | D86096 |
| 718_at | Protease, serine, 11 (IGF binding) | 1.1 | 1.2 | 1.0 | 2.8 | 1.7 | <i>PRSS11</i> | D87258 |
| 39255_at | Protein C (inactivator of coagulation factors Va and VIIIa) | 0.5 | 0.7 | 0.5 | 0.7 | 0.6 | <i>PROC</i> | X02750 |
| 647_at | Protein C receptor, endothelial (EPCR) | 2.7 | 1.7 | 1.4 | 2.1 | 3.1 | <i>PROCR</i> | L35545 |
| 37432_g_at | Protein inhibitor of activated STAT, 2 | 1.2 | 1.9 | 1.7 | 2.4 | 2.0 | <i>PIAS2</i> | AF077953 |
| 1810_s_at | Protein kinase C, delta | 1.5 | 1.9 | 1.3 | 1.5 | 2.1 | <i>PRKCD</i> | D10495 |
| 34342_s_at | Secreted phosphoprotein 1 (osteopontin, bone sialoprotein I, early T-lymphocyte activation 1) | 13.9 | 1.8 | 2.2 | 1.4 | 5.6 | <i>SPPI</i> | AF052124 |
| 32275_at | Secretory leukocyte protease inhibitor (antileukoproteinase) | 1.2 | 2.1 | 2.9 | 2.2 | 1.8 | <i>SLPI</i> | X04470 |
| 40366_at | Selectin P (granule membrane protein 140 kDa, antigen CD62) | 1.7 | 5.5 | 3.7 | 1.1 | 4.4 | <i>SELP</i> | M25322 |

Table IV. Continued

| Affymetrix ID | Gene title | Ratio of expression levels (treated/untreated) | | | | | Gene symbol | GenBank |
|-----------------------------|---|--|-------|-----------------|--------|---------------|-----------------|----------|
| | | Kidney | Liver | Pituitary gland | Spleen | Thyroid gland | | |
| <i>Acute-phase response</i> | | | | | | | | |
| 33825_at | Serine (or cysteine) proteinase inhibitor, clade A (alpha-1 antiproteinase, antitrypsin), member 3 | 3.6 | 2.0 | 3.3 | 2.0 | 2.4 | <i>SERPINA3</i> | X68733 |
| 33305_at | Serine (or cysteine) proteinase inhibitor, clade B (ovalbumin), member 1 | 4.4 | 1.5 | 4.6 | 1.2 | 12.7 | <i>SERPINB1</i> | M93056 |
| 32103_at | Serine (or cysteine) proteinase inhibitor, clade F (alpha-2 antiplasmin, pigment epithelium derived factor), member 2 | 1.2 | 1.1 | 1.5 | 2.3 | 1.1 | <i>SERPINF2</i> | M20786 |
| 39775_at | Serine (or cysteine) proteinase inhibitor, clade G (C1 inhibitor), member 1, (angioedema, hereditary) | 1.0 | 1.1 | 1.5 | 1.0 | 1.1 | <i>SERPING1</i> | X54486 |
| 40109_at | Serum response factor (<i>c-fos</i> serum response element-binding transcription factor) | 1.6 | 1.6 | 1.2 | 1.2 | 1.8 | <i>SRF</i> | J03161 |
| 1563_s_at | Tumor necrosis factor receptor superfamily, member 1A | 1.6 | 1.8 | 1.6 | 2.2 | 1.7 | <i>TNFRSF1A</i> | M58286 |
| 36988_at | Tumor necrosis factor, alpha-induced protein 1 (endothelial) | 1.7 | 1.5 | 1.8 | 1.6 | 2.1 | <i>TNFAIP1</i> | M80783 |
| 1519_at | <i>v-ets</i> erythroblastosis virus E26 oncogene homolog 2 (avian) | 2.9 | 3.0 | 1.6 | 2.6 | 3.4 | <i>ETS2</i> | J04102 |
| 1916_s_at | <i>v-fos</i> FBJ murine osteosarcoma viral oncogene homolog | 2.0 | 6.3 | 2.1 | 1.6 | 3.7 | <i>FOS</i> | V01512 |
| 37724_at | <i>v-myc</i> myelocytomatosis viral oncogene homolog (avian) | 8.1 | 3.4 | 1.6 | 1.6 | 1.3 | <i>MYC</i> | V00568 |
| 607_s_at | von Willebrand factor | 1.4 | 1.0 | 3.4 | 2.9 | 1.4 | <i>VWF</i> | M10321 |
| <i>Immune response</i> | | | | | | | | |
| 1796_s_at | B-cell CLL/lymphoma 3 | 1.2 | 1.8 | 1.2 | 2.0 | 1.2 | <i>BCL3</i> | U05681 |
| 40091_at | B-cell CLL/lymphoma 6 (zinc finger protein 51) | 2.3 | 5.2 | 3.5 | 1.6 | 1.7 | <i>BCL6</i> | U00115 |
| 2036_s_at | CD44 antigen (homing function and Indian blood group system) | 2.6 | 1.7 | 1.9 | 1.2 | 1.1 | <i>CD44</i> | M59040 |
| 37536_at | CD83 antigen (activated B lymphocytes, immunoglobulin superfamily) | 0.5 | 0.8 | 0.9 | 0.7 | 0.7 | <i>CD83</i> | Z11697 |
| 875_g_at | Chemokine (C-C motif) ligand 2 | 2.1 | 1.6 | 1.0 | 1.1 | 2.9 | <i>CCL2</i> | M26683 |
| 823_at | Chemokine (C-X3-C motif) ligand 1 | 1.2 | 1.1 | 1.1 | 1.4 | 1.4 | <i>CX3CL1</i> | U84487 |
| 34344_at | Inhibitor of kappa light polypeptide gene enhancer in B-cells, kinase complex-associated protein | 0.8 | 0.6 | 0.6 | 0.8 | 0.8 | <i>IKBKAP</i> | AF044195 |
| 120_at | Integrin, alpha 1 | 1.1 | 1.7 | 1.7 | 1.9 | 1.0 | <i>ITGA1</i> | X68742 |
| 41005_at | Integrin, alpha 8 | 1.3 | 2.2 | 4.0 | 1.1 | 1.8 | <i>ITGA8</i> | L36531 |
| 32808_at | Integrin, beta 1 (fibronectin receptor, beta polypeptide, antigen CD29 includes MDF2, MSK12) | 1.2 | 1.3 | 1.1 | 2.1 | 1.3 | <i>ITGB1</i> | X07979 |
| 37952_at | Integrin, beta 3 (platelet glycoprotein IIIa, antigen CD61) | 3.8 | 2.9 | 2.1 | 3.6 | 2.2 | <i>ITGB3</i> | M35999 |
| 32640_at | Intercellular adhesion molecule 1 (CD54), human rhinovirus receptor | 3.7 | 3.5 | 5.0 | 1.9 | 3.6 | <i>ICAM1</i> | M24283 |
| 38453_at | Intercellular adhesion molecule 2 | 1.2 | 1.1 | 2.6 | 1.1 | 1.2 | <i>ICAM2</i> | X15606 |
| 676_g_at | Interferon-induced transmembrane protein 1 (9-27) | 1.7 | 2.3 | 3.9 | 1.3 | 2.2 | <i>IFITM1</i> | J04164 |

Table IV. Continued

| Affymetrix ID | Gene title | Ratio of expression levels (treated/untreated) | | | | | Gene symbol | GenBank |
|------------------------------|---|--|-------|-----------------|--------|---------------|-----------------|----------|
| | | Kidney | Liver | Pituitary gland | Spleen | Thyroid gland | | |
| <i>Immune response</i> | | | | | | | | |
| 41745_at | Interferon-induced transmembrane protein 3 (1–8U) | 2.5 | 2.7 | 2.1 | 1.6 | 3.7 | <i>IFITM3</i> | X57352 |
| 669_s_at | Interferon regulatory factor 1 | 4.6 | 2.3 | 4.2 | 1.4 | 3.6 | <i>IRF1</i> | L05072 |
| 36412_s_at | Interferon regulatory factor 7 | 2.2 | 2.7 | 1.7 | 1.4 | 2.8 | <i>IRF7</i> | U53831 |
| 1358_s_at | Interferon, alpha-inducible protein (clone IFI-6-16) | 2.2 | 6.4 | 1.1 | 5.9 | 1.6 | <i>GIP3</i> | U22970 |
| 37641_at | Interferon-induced protein 44 | 1.1 | 1.8 | 1.4 | 1.8 | 1.8 | <i>IFI44</i> | D28915 |
| 915_at | Interferon-induced protein with tetratricopeptide repeats 1 | 1.1 | 2.1 | 1.9 | 1.8 | 2.7 | <i>IFIT1</i> | M24594 |
| 36472_at | N-myc (and STAT) interactor | 1.9 | 1.4 | 1.8 | 1.0 | 1.2 | <i>NMI</i> | U32849 |
| 40822_at | Nuclear factor of activated T-cells, cytoplasmic, calcineurin-dependent 3 | 0.8 | 0.6 | 1.0 | 0.9 | 0.5 | <i>NFATC3</i> | L41067 |
| 37397_at | Platelet/endothelial cell adhesion molecule (CD31 antigen) | 1.1 | 2.4 | 1.6 | 1.5 | 1.0 | <i>PECAMI</i> | L34657 |
| 33823_at | Scavenger receptor class B, member 2 | 1.2 | 1.1 | 1.1 | 1.3 | 1.4 | <i>SCARB2</i> | D12676 |
| 39708_at | Signal transducer and activator of transcription 3 (acute-phase response factor) | 1.6 | 1.6 | 2.3 | 1.8 | 2.2 | <i>STAT3</i> | L29277 |
| 38994_at | Suppressor of cytokine signaling 2 | 2.6 | 1.3 | 1.4 | 1.6 | 1.3 | <i>SOCS2</i> | AF037989 |
| 32669_at | Suppressor of cytokine signaling 5 | 1.3 | 1.4 | 1.9 | 1.1 | 1.2 | <i>SOCS5</i> | AB014571 |
| 31557_at | Thymosin, beta 4, X-linked | 1.2 | 1.2 | 1.5 | 1.0 | 1.2 | <i>TMSB4X</i> | M17733 |
| 41433_at | Vascular cell adhesion molecule 1 | 2.5 | 1.5 | 6.4 | 1.2 | 2.0 | <i>VCAM1</i> | M73255 |
| <i>Repair</i> | | | | | | | | |
| 32307_s_at | Collagen, type I, alpha 2 | 1.5 | 2.2 | 1.1 | 1.7 | 1.6 | <i>COL1A2</i> | V00503 |
| 32488_at | Collagen, type III, alpha 1 (Ehlers–Danlos syndrome type IV, autosomal dominant) | 1.8 | 2.5 | 4.6 | 2.8 | 1.8 | <i>COL3A1</i> | X14420 |
| 39333_at | Collagen, type IV, alpha 1 | 2.9 | 1.8 | 1.4 | 3.6 | 2.0 | <i>COL4A1</i> | M26576 |
| 36659_at | Collagen, type IV, alpha 2 | 1.9 | 1.6 | 1.4 | 2.6 | 2.0 | <i>COL4A2</i> | X05610 |
| 38722_at | Collagen, type VI, alpha 1 | 2.2 | 1.6 | 1.6 | 2.0 | 1.1 | <i>COL6A1</i> | X15880 |
| 38077_at | Collagen, type VI, alpha 3 | 1.4 | 1.3 | 1.3 | 1.5 | 1.2 | <i>COL6A3</i> | X52022 |
| 996_at | Fibroblast growth factor 1 (acidic) | 0.6 | 0.6 | 0.6 | 0.8 | 0.4 | <i>FGF1</i> | X59065 |
| 36184_at | Procollagen-lysine, 2-oxoglutarate 5-dioxygenase (lysine hydroxylase, Ehlers–Danlos syndrome type VI) | 1.5 | 1.2 | 1.5 | 2.1 | 1.9 | <i>PLOD</i> | L06419 |
| 224_at | Transforming growth factor beta-inducible early growth response | 1.0 | 1.1 | 1.8 | 1.1 | 1.4 | <i>TIEG</i> | S81439 |
| 1693_s_at | Tissue inhibitor of metalloproteinase 1 (erythroid-potentiating activity, collagenase inhibitor) | 8.9 | 21 | 1.5 | 7.2 | 6.2 | <i>TIMP1</i> | D11139 |
| 1767_s_at | Transforming growth factor beta 3 | 1.2 | 2.4 | 1.8 | 1.7 | 2.5 | <i>TGFB3</i> | X14885 |
| 1897_at | Transforming growth factor beta receptor III (beta glycan, 300 kDa) | 2.3 | 1.3 | 1.1 | 1.4 | 1.2 | <i>TGFBR3</i> | L07594 |
| <i>Programmed cell death</i> | | | | | | | | |
| 1497_at | Lymphotoxin beta receptor (TNFR superfamily, member 3) | 2.0 | 1.2 | 1.6 | 3.6 | 2.3 | <i>LTBR</i> | L04270 |
| 1563_s_at | Tumor necrosis factor receptor superfamily, member 1A | 1.6 | 1.8 | 1.6 | 2.2 | 1.7 | <i>TNFRSF1A</i> | M58286 |
| 1911_s_at | Growth arrest and DNA-damage-inducible, alpha | 2.6 | 1.2 | 1.3 | 2.3 | 2.0 | <i>GADD45A</i> | M60974 |
| 195_s_at | Caspase 4, apoptosis-related cysteine protease | 5.6 | 3.0 | 4.7 | 1.6 | 1.9 | <i>CASP4</i> | U28014 |
| 38281_at | Caspase 7, apoptosis-related cysteine protease | 1.8 | 1.2 | 2.1 | 1.1 | 1.8 | <i>CASP7</i> | U67319 |

Table IV. Continued

| Affymetrix ID | Gene title | Ratio of expression levels (treated/untreated) | | | | | Gene symbol | GenBank |
|------------------------------|---|--|-------|-----------------|--------|---------------|-------------|----------|
| | | Kidney | Liver | Pituitary gland | Spleen | Thyroid gland | | |
| <i>Programmed cell death</i> | | | | | | | | |
| 2092_s_at | Secreted phosphoprotein 1 (osteopontin, bone sialoprotein I, early T-lymphocyte activation 1) | 11.0 | 1.6 | 2.8 | 1.6 | 2.0 | SPP1 | J04765 |
| 34342_s_at | Secreted phosphoprotein 1 (osteopontin, bone sialoprotein I, early T-lymphocyte activation 1) | 13.9 | 1.8 | 2.2 | 1.4 | 5.6 | SPP1 | AF052124 |
| 31888_s_at | Pleckstrin homology-like domain, family A, member 2 | 1.2 | 1.7 | 2.4 | 0.9 | 1.5 | PHLDA2 | AF001294 |
| 34185_at | Poly(rC) binding protein 4 | 0.5 | 0.6 | 0.8 | 0.5 | 0.4 | PCBP4 | W22541 |
| 39020_at | CD27-binding (Siva) protein | 0.8 | 0.7 | 0.7 | 0.8 | 0.8 | SIVA | U82938 |
| 41349_at | Presenilin 2 (Alzheimer disease 4) | 1.6 | 1.3 | 1.2 | 1.2 | 1.9 | PSEN2 | L43964 |
| 875_g_at | Chemokine (C-C motif) ligand 2 | 2.1 | 1.6 | 1.0 | 1.1 | 2.9 | CCL2 | M26683 |

by compound B treatment, nor did we detect significant changes in TNF-receptor-associated factor (TRAF) signaling through NF- κ B. Some genes involved in programmed cell death were dysregulated in most tissues by compound B, but we did not see the hallmark caspases 3 and 8 (Table III). This effect could be attributed to an activation of TNF-signaling pathway through death domain bearing receptor-associated proteins. While IL-6 like cytokines have antiapoptotic activity (40,41), it could not be excluded that the observed changes may reflect direct or indirect effects of this cytokine family. Members of the IL-6 cytokine family bind to receptor complexes comprising combinations of specific signaling receptor subunits and a common subunit, gp130. Downstream signaling events involve, among others, the JAK/STAT pathway, SOCS, and the Ras/MAPK pathway, some of which were affected by treatment with compound B. Oncostatin M receptor (IL-6 receptor) and tissue inhibitor of metalloproteinase-1 (TIMP-1) were up-regulated in all tissues. Tissue inhibitor of metalloproteinase-1, a target gene of LIF (42), was particularly overexpressed in the liver (Tables III and IV).

Because of the overall lack of upstream members of the TNF or LPS-stimulated signaling pathway in our gene list on one hand, and the presence of a number of members of the IL-6-family pathway, we came to the conclusion that the gene expression signature was not consistent with induction of the LPS or the TNF signaling cascades. Instead, we speculated that compound B could be a cytokine that may be downstream of those signaling pathways, with the ability to elicit acute phase response. Based on the components of the signaling pathways represented by gene expression signature, it was surmised that compound B was most likely a member of the IL-6 family of cytokines rather than an LPS-like or TNF-like molecule. In fact, deblinding revealed that compound B was LIF.

DISCUSSION

Microarray gene expression profiles provide a readout of the concerted regulation of the transcriptome and may be considered fingerprints of cellular physiology (43). The approach we describe here, VeloceGenomics, provides a

detailed overview of the early transcriptional events induced by any potential drug-like compound, but it may also include the secondary responses that manifest in the form of metabolic and physiologic changes in the animal. An example of the usefulness of our strategy was demonstrated by showing that it was possible for data analysts masked to treatment conditions to determine the biologic function or activity of compounds based solely on multiorgan whole transcriptome signature analysis. The goal of the exercise was not to determine precisely the identity of the compound but rather to test whether the gene expression profiles allowed the positioning of the compounds into classes of activity, could suggest a mode of action, and could propose possible therapeutic indications.

The gene expression signatures exhibited by each group of animals allowed us to identify compound A as having a GH-like activity and compound B as having activity related to proinflammatory cytokines. Indeed, after deblinding, compound A was revealed to be a somatostatin analog (SOM230) and compound B to be LIF. In each case, the expression patterns provided clues as to what pathways and activities were being regulated. For SOM230, the nature of the changes suggested the involvement of the glucagon/insulin axes. The change in expression of various receptors suggested that compound A was acting along the lines of a ligand and stimulating many downstream pathways rather than acting as a downstream effector itself. For compound B, the gene expression signature clearly implicated the inflammatory response. More thorough evaluations ruled out certain possibilities (e.g., LPS) and suggested others as more plausible (i.e., IL-6-like cytokine activity).

The VeloceGenomics method may be applied to virtually any organism used in preclinical settings and is not limited to the analysis of gene expression data. Indeed, the process may be enhanced by collecting additional data—physiologic, biochemical, hematologic—as complementary information, such that an entire picture of the physiologic responses to a compound can be gained in a single appropriately designed experiment. The VeloceGenomics approach provides an early *in vivo* pharmacologic evaluation of efficacy and safety. Information garnered from these

experiments can lead to testable hypotheses of the mode of action and the biologic activity of the compound in focused experiments. The vast molecular readouts obtained from a single *in vivo* multiorgan transcriptome study can support a multitude of efforts in drug discovery research, including identifying and validating targets, selecting lead compounds, identifying new clinical indications for existing drugs, discovering biomarkers, and elucidating mechanisms of action. The VeloceGenomics approach combines the power of systems biology (physiology) and functional genomics (when applied to proteins or genes) to produce an innovative strategy to investigate the actions of compounds on an organism-wide level of complexity. Computational methods, such as structure-based design, have made significant contributions in the realm of synthetic chemical synthesis; however, such methods cannot replace empirical testing to establish the actual biologic activity of compounds (44). Our approach of *in vivo* global genomics is a strategy to capture quantitative data from such an empirical approach that has the potential to elucidate the entire spectrum of biologic activity of any compound.

The VeloceGenomics process may be used to derive the biologic function or action of any molecule or gene. Small molecules, proteins, and natural products—even genes through *in vivo* naked DNA injections—are all amenable to this strategy (45,46). Compounds can be applied to VeloceGenomics screening in the absence of any predetermined biologic selection criteria. The resultant *in vivo* organism-wide pattern of transcriptome expression data provides an overview of the activities affected at the molecular and organismal levels. The accumulation of information in different organs not only helps to elucidate the mode of action, but it can provide also valuable insight into the potential therapeutic usefulness or toxicologic consequences of any molecule by providing a comprehensive reconstruction of the compound-induced perturbations throughout the entire organism. *In vivo* gene expression analysis may reveal the extent to which a compound acts at more than one target and in more than one target organ (5); both factors may be critical in determining product safety.

Targets of many currently marketed drugs were identified from pharmacology (physiology) studies rather than from a direct molecular approach (2). Our *in vivo* global genomics approach combines a physiologic approach with a simultaneous effort to evaluate the molecular pathways impacted by treatment. The physiology of the whole organism affects how a compound acts *in vivo*, and the *in vivo* gene expression profile reveals the molecular targets and the metabolic and biochemical pathways involved in that compound's *in vivo* biologic activity (2). The VeloceGenomics process is suitable for several stages in the drug discovery and drug development process. The phase of the process at which our strategy is introduced may reflect the type of molecule under evaluation. For example, novel proteins or genes may be subjected to the VeloceGenomics approach early in the evaluation process. In the case of small molecule chemical screening, the VeloceGenomics process may be invoked once a limited set of lead compounds is identified based on high-throughput evaluations of compound libraries.

In the past three decades, drug discovery has shifted from the extensive use of animal studies (classical pharma-

cology) to high-throughput *in vitro* screening systems using a target-oriented approach (5). However, it has been repeatedly demonstrated that the *in vitro* testing of compounds leads to promising drug candidates that often fail to show the expected or predicted efficacy *in vivo* (44). A recent publication has elegantly demonstrated the limitations of *in vitro* models in which detection of the number of different proteins expressed *in vivo* by endothelial cells of the lung microvasculature was approximately 2.5-fold greater than the number of proteins expressed by the same cells *in vitro* (7). These results have profound implications for drug discovery using *in vitro* cell-based assays when testing for the biologic activity of compounds. If, as in this example, the *in vitro* system expresses far fewer proteins, the suggestion is that not all relevant pathways may be expressed *in vitro* compared with the same cells growing under *in vivo* conditions. Thus, the *in vitro* system may be an inaccurate representation of the biochemical and metabolic pathways active in the *in vivo* condition. However, at the *in vivo* level, the congruence between animal physiology and biochemistry is substantially valid when compared with human biochemistry and physiology (6). Furthermore, *in vitro* screening and tests for biologic activity lack aspects of functional kinetics. As such, *in vitro* screening lacks the aspects of systems biology in which the various molecular, biochemical, and physiologic pathways interact and interconnect kinetically (6). The VeloceGenomics approach addresses these concerns.

In addition, many compounds undergo metabolic conversion to generate the biologically active drug species (or, in some cases, toxic metabolites). The discovery of such a compound would be dependent on its interaction with a metabolically competent test system. Hence, the therapeutic effect of the drug would depend on its interaction with the organism; this interaction cannot take place in an *in vitro* system (11).

Attrition is one of the central issues confronting drug discovery and development. Most attrition that occurs late in drug development is attributed to lack of *in vivo* efficacy or to problems with absorption, distribution, metabolism, excretion, or toxicology (8). Predicting the biologic success or failure of a compound is critical in pharmaceutical discovery, where the guiding principle during research and development is to fail early and cheap. The ability to reconcile or unify genetics and physiology can play an important role in this process (48). Suggestions to improve the attrition rate include (a) strong evidence for mechanism (mode) of action, (b) elimination of compounds that have mechanism-based toxicity, (c) identification of biomarkers that signal correct dosing and on-target action, and (d) use of appropriate animal models for efficacy testing (8). The strategy presented by VeloceGenomics addresses each of these points and may be used to identify risk during the preclinical stages of drug discovery through an understanding of the mechanism of action and drug-like activity of a compound in a physiologically relevant setting (8,9). By refining or narrowing the scope of the *in vivo* global genomics approach—for instance, by using animal models of disease—the efficacy, potency, toxicity, and mechanism of action can be assessed in one study. Although this more focused approach may reduce the amount of information generated from an *in vivo* global genomics study, it does lend itself to focused drug discovery

(3). Rather, the value of the data would depend on the animal model having relevance to the human disease or to the question being addressed (6). In many instances, one can generate preliminary knowledge regarding these points in a well-designed *in vivo* study. Because the VeloceGenomics strategy has the potential to reveal a compound's mechanism of action, it can assist in the choice of the best animal models and disease models to assess efficacy and safety.

In vivo microarray experiments help in elucidating the underlying principles of *in vivo* drug action; however, there are limitations. Compounds with poor pharmacokinetics may be unable to generate reliable *in vivo* transcriptome profiles and, hence, may fail to reveal information hidden in RNA expression levels. Furthermore, biologic activities caused by translational activity and posttranslational modifications, such as protein phosphorylation, are not seen at the transcript level.

Rapid advances are being made in microarray-related technologies and information databases. The availability of more human tissue transcriptome profiles representing healthy and pathologic states will greatly improve concordance between animal and human tissue transcriptomes. Human pathologic tissue signatures will be used (and are already used, where available) to evaluate the effect of compounds in preclinical testing. For example, human cancer tissue transcript expression profiles may be compared before and after treatment with the transcript expression profile of an animal model counterpart. Establishing databases of treatment signatures based on real treatment samples will substantially improve the predicative power of *in vivo* preclinical testing.

It has been estimated that 12,000–14,000 genes encode secreted proteins in the human genome (3). If only 1–2% of these proteins become drugs, that would translate into 120–280 novel biopharmaceutics (3). Biologicals have a high success rate (approximately 24%) in passing through clinical development and registration (8). The growth of biotechnology-based drugs has been impressive. In 1982, recombinant insulin was registered. By 2000, 60 protein-based drugs were introduced to the market (47,49). The VeloceGenomics strategy outlined in this work would most quickly apply to the search for novel protein-based drugs.

CONCLUSION

In summary, VeloceGenomics *in vivo* whole transcriptome analysis attempts to answer in one study the following questions. (a) Is the compound worth further investigation? (b) What physiologic pathways are affected by treatment (i.e., mechanism of action)? (c) What are the potential therapeutic indications? (d) What are the potential safety concerns and adverse effects? Furthermore, through *in vivo* transcriptome analysis, additional targets for therapeutic intervention may be revealed. This information provides an important link back to disease research and discovery programs charged with the task of identifying valid, “drugable” targets for high-throughput screens. The drug discovery approach described as VeloceGenomics is a strategy to generate and analyze a vast amount of data from single *in vivo* studies to derive knowledge pertaining to a compound's mode of action, biologic activity, safety implications, and potential therapeutic indications. Use of an *in vivo*

system maintains the integrity of all physiologic interactions among the different organs, tissues, and cells, and any cellular pathway or target can be analyzed under physiologically relevant conditions.

ACKNOWLEDGMENTS

The authors thank Nicole Hartmann for expert technical assistance and Mark Bossie, PhD, and Maribeth Bogush, PhD, for assistance in preparation of the manuscript. This work was funded by Novartis Pharma AG.

REFERENCES

1. D. L. Gerhold, R. V. Jensen, and S. R. Gullans. Better therapeutics through microarrays. *Nat. Genet.* **32**:547–551 (2002).
2. M. A. Lindsay. Target discovery. *Nat. Rev., Drug Discov.* **2**:831–838 (2003).
3. J. Drews. Drug discovery: a historical perspective. *Science* **287**:1960–1964 (2000).
4. C. Debouck and P. N. Goodfellow. DNA microarrays in drug discovery and development. *Nat. Genet.* **21**:48–50 (1999).
5. H. Kubinyi. Drug research: myths, hype and reality. *Nat. Rev., Drug Discov.* **2**:665–668 (2003).
6. D. F. Horrobin. Modern biomedical research: an internally self-consistent universe with little contact with medical reality? *Nat. Rev., Drug Discov.* **2**:151–154 (2003).
7. E. Durr, J. Yu, K. M. Krasinska, L. A. Carver, J. R. Yates, J. E. Testa, P. Oh, and J. E. Schnitzer. Direct proteomic mapping of the lung microvascular endothelial cell surface *in vivo* and in cell culture. *Nat. Biotechnol.* **22**:985–992 (2004).
8. I. Kola and J. Landis. Can the pharmaceutical industry reduce attrition rates? *Nat. Rev., Drug Discov.* **3**:711–715 (2004).
9. H. Ellinger-Ziegelbauer, B. Stuart, B. Wahle, W. Bomann, and H. J. Ahr. Characteristic expression profiles induced by genotoxic carcinogens in rat liver. *Toxicol. Sci.* **77**:19–34 (2004).
10. Y. C. Patel. Somatostatin and its receptor family. *Front. Neuroendocrinol.* **20**:157–198 (1999).
11. B. B. Fredholm, W. W. Fleming, P. M. Vanhoutte, and T. Godfraind. The role of pharmacology in drug discovery. *Nat. Rev., Drug Discov.* **1**:237–238 (2002).
12. P. Chomczynski and N. Sacchi. Single-step method of RNA isolation by acid guanidinium thiocyanate–phenol–chloroform extraction. *Anal. Biochem.* **162**:156–159 (1987).
13. D. J. Lockhart, H. Dong, M. C. Byrne, M. T. Follettie, M. V. Gallo, M. S. Chee, M. Mittmann, C. Wang, M. Kobayashi, H. Horton, and E. L. Brown. Expression monitoring by hybridization to high-density oligonucleotide arrays. *Nat. Biotechnol.* **14**:1675–1680 (1996).
14. G. Liu, A. E. Loraine, R. Shigeta, M. Cline, J. Cheng, V. Valmeekam, S. Sun, D. Kulp, and M. A. Siani-Rose. NetAffx: affymetrix probesets and annotations. *Nucleic Acids Res.* **31**:8–86 (2003).
15. K. C. Leung and K. K. Ho. Measurement of growth hormone, insulin-like growth factor I and their binding proteins: the clinical aspects. *Clin. Chim. Acta* **313**:119–123 (2001).
16. M. Giusti, L. Bocca, T. Florio, A. Corsaro, R. Spaziente, G. Schettini, and F. Minuto. *In vitro* effect of recombinant leptin and expression of leptin receptors on growth hormone-secreting human pituitary adenomas. *Clin. Endocrinol.* **57**:449–455 (2002).
17. L. Cuttler, P. A. Birkenbach, and M. Szabo. The effect of age on prostaglandin E2 stimulation of growth hormone release from cultured rat pituitary cells. *Endocrinology* **124**:661–666 (1989).
18. S. Siehler and D. Hoyer. Characterisation of human recombinant somatostatin receptors. 3. Modulation of adenylate cyclase activity. *Naunyn-Schmiedeberg's Arch. Pharmacol.* **360**:510–521 (1999).

19. M. Akbar, F. Okajima, H. Tomura, M. A. Majid, Y. Yamada, S. Seino, and Y. Kondo. Phospholipase C activation and Ca²⁺ mobilization by cloned human somatotropin receptor subtypes 1–5, in transfected COS-7 cells. *FEBS Lett.* **348**:192–196 (1994).
20. L. N. Møller, C. E. Stidsen, B. Hartmann, and J. J. Holst. Somatostatin receptors. *Biochim. Biophys. Acta* **1616**:1–84 (2003).
21. M. Tallent, G. Liapakis, A. M. O'Carroll, S. J. Lolait, M. Dichter, and T. Reisine. Somatostatin receptor subtypes sstr2 and sstr5 couple negatively to an L-type Ca²⁺ current in the pituitary cell line AtT-20. *Neuroscience* **71**:1073–1081 (1996).
22. H. J. Kreienkamp, H. H. Honck, and D. Richter. Coupling of rat somatostatin receptor subtypes to a G-protein gated inwardly rectifying potassium channel (GIRK1). *FEBS Lett.* **419**:92–94 (1997).
23. L. Buscail, N. Delsque, J. P. Esteve, N. Saint-Laurent, H. Prats, P. Clerc, P. Robberecht, G. I. Bell, C. Liebow, A. V. Schally, N. Vaysse, and C. Susini. Stimulation of tyrosine phosphatase and inhibition of cell proliferation by somatostatin analogues: mediation by human somatostatin receptor subtypes SSTR1 and SSTR. *Proc. Natl. Acad. Sci. USA* **91**:2315–2319 (1994).
24. J. Held-Feindt, F. Forstreuter, T. Pufe, and R. Mentlein. Influence of the somatostatin receptor sst2 on growth factor signal cascade in human glioma cells. *Mol. Brain Res.* **87**:12–21 (2001).
25. M. G. Cattaneo, D. Amoroso, G. Gussoni, A. M. Sanguini, and L. M. Vicentini. A somatostatin analog inhibits MAP kinase activation and cell proliferation in human neuroblastoma and in human small cell lung carcinoma cell lines. *FEBS Lett.* **397**:164–168 (1996).
26. H. Lahlou, J. Guillermet, M. Hortala, F. Vernejoul, S. Pyronnet, C. Bousquet, and C. Susini. Molecular signaling of somatostatin receptors. *Ann. N.Y. Acad. Sci.* **1014**:121–131 (2004).
27. G. I. Bell, K. Yasuda, H. Kong, S. F. Law, K. Raynor, and T. Reisine. Molecular biology of somatostatin receptors. *Ciba Found. Symp.* **190**:65–79 (1995).
28. M. H. Regenmortel. Are there two distinct research strategies for developing biologically active molecules: rational design and empirical selection? *J. Mol. Recognit.* **13**:1–4 (2000).
29. J. E. Parrillo. Pathogenetic mechanisms of septic shock. *N. Engl. J. Med.* **328**:1471–1477 (1993).
30. P. C. Heinrich, I. Behrmann, S. Haan, H. M. Hermanns, G. Muller-Newen, and F. Schaper. Principles of interleukin (IL)-6-type cytokine signaling and its regulation. *Biochem. J.* **374**:1–20 (2003).
31. R. L. Modlin, H. D. Brightbill, and P. J. Godowski. The toll of innate immunity on microbial pathogens. *N. Engl. J. Med.* **340**:1834–1835 (1999).
32. K. Miyake. Innate recognition of lipopolysaccharide by CD14 and toll-like receptor 4-MD-2: unique roles for MD-2. *Int. Immunopharmacol.* **3**:119–128 (2003).
33. E. M. Palsson-McDermott and L. A. O'Neill. Signal transduction by the lipopolysaccharide receptor, toll-like receptor-4. *Immunology* **113**:153–162 (2004).
34. T. Ikezoe, Y. Yang, D. Heber, H. Taguchi, and H. P. Koeffler. PC-SPES: a potent inhibitor of nuclear factor- κ B rescues mice from lipopolysaccharide-induced septic shock. *Mol. Pharmacol.* **64**:1521–1529 (2003).
35. R. D. Fannin, J. T. Auman, M. E. Bruno, S. O. Sieber, S. M. Ward, C. J. Tucker, B. A. Merrick, and R. S. Paules. Differential gene expression profiling in whole blood during acute systemic inflammation in lipopolysaccharide-treated rats. *Physiol. Genomics* **21**:92–104 (2005).
36. K. Jatta, D. Wagsater, L. Norgren, B. Stenberg, and A. Sirsjo. Lipopolysaccharide-induced cytokine and chemokine expression in human carotid lesions. *J. Vasc. Res.* **42**:266–271 (2005).
37. H. Bjorkbacka, K. A. Fitzgerald, F. Huet, X. Li, J. A. Gregory, M. A. Lee, C. M. Ordija, N. E. Dowley, D. T. Golenbock, and M. W. Freeman. The induction of macrophage gene expression by LPS predominantly utilizes Myd88-independent signaling cascades. *Physiol. Genomics* **19**:319–330 (2004).
38. J. Inoue, T. Ishida, N. Tsukamoto, N. Kobayashi, A. Naito, S. Azuma, and T. Yamamoto. Tumor necrosis factor receptor-associated factor (TRAF) family: adapter proteins that mediate cytokine signaling. *Exp. Cell Res.* **254**:14–24 (2000).
39. A. K. Garg and B. B. Aggarwal. Reactive oxygen intermediates in TNF signaling. *Mol. Immunol.* **39**:509–517 (2002).
40. H. Negoro, E. Oh, K. Tone, Y. Kunisada, K. Fujio, T. Walsh, Kishimoto, and K. Yamauchi-Takahara. Glycoprotein 130 regulates cardiac myocyte survival in doxorubicin-induced apoptosis through phosphatidylinositol 3-kinase/Akt phosphorylation and Bcl-xL/caspase-3 interaction. *Circulation* **103**:555–561 (2001).
41. M. Philip, D. A. Rowley, and H. Schreiber. Inflammation as a tumor promoter in cancer induction. *Semin. Cancer Biol.* **14**:433–439 (2004).
42. G. Florholmen, K. B. Andersson, A. Yndestad, B. Austbo, U. L. Henriksen, and G. Christensen. Leukaemia inhibitory factor alters expression of genes involved in rat cardiomyocyte energy metabolism. *Acta Physiol. Scand.* **180**:133–142 (2004).
43. E. C. Gunther, D. J. Stone, R. W. Gerwien, P. Bento, and M. P. Heyes. Prediction of clinical drug efficacy by classification of drug-induced genomic expression profiles *in vitro*. *Proc. Natl. Acad. Sci. USA* **100**:9608–9613 (2003).
44. M. Williams. A return to the fundamentals of drug discovery? *Curr. Opin. Investig. Drugs* **5**:29–33 (2004).
45. S. F. Alino, A. Crespo, and F. Dasi. Long-term therapeutic levels of human alpha-1 antitrypsin in plasma after hydrodynamic injection of nonviral DNA. *Gene Ther.* **10**:1672–1679 (2003).
46. J. M. Kim, S. H. Ho, W. Hahn, J. G. Jeong, E. J. Park, H. J. Lee, S. S. Yu, C. S. Lee, Y. W. Lee, and S. Kim. Electro-gene therapy of collagen-induced arthritis by using an expression plasmid for the soluble p75 tumor necrosis factor receptor-Fc fusion protein. *Gene Ther.* **10**:1216–1224 (2003).
47. S. Lien and H. B. Lowman. Therapeutic peptides. *Trends Biotechnol.* **21**:556–562 (2003).
48. G. Duyk. Attrition and translation. *Science* **302**:603–605 (2003).
49. M. Kleinberg and K. Wilkinson-Mosdell. Current and future considerations for the new classes of biologicals (Primer). *Am. J. Health-Syst. Pharm.* **61**:695–708 (2004).